Commentary

Data Generated by Quantitative Liquid Chromatography-Mass Spectrometry Proteomics Are Only the Start and Not the Endpoint: Optimization of Quantitative Concatemer-Based Measurement of Hepatic Uridine-5′-Diphosphate–Glucuronosyltransferase Enzymes with Reference to Catalytic Activity[S]

Brahim Achour, Alyssa Dantonio, Mark Niosi, Jonathan J. Novak, Zubida M. Al-Majdoub, Theunis C. Goosen, Amin Rostami-Hodjegan, and Jill Barber

Centre for Applied Pharmacokinetic Research, Division of Pharmacy and Optometry, University of Manchester, Manchester, United Kingdom (B.A., Z.M.A.-M., A.R.-H., J.B.); Department of Pharmacokinetics, Dynamics, and Metabolism, Pfizer Inc., Groton, Connecticut (A.D., M.N., J.J.N., T.C.G.); and Simcyp Limited (a Certara Company), Blades Enterprise Centre, Sheffield, United Kingdom (A.R.-H.)

ABSTRACT

Quantitative proteomic methods require optimization at several stages, including sample preparation, liquid chromatography–tandem mass spectrometry (LC-MS/MS), and data analysis, with the final analysis stage being less widely appreciated by end-users. Previously reported measurement of eight uridine-5′-diphospho-glucuronosyltransferases (UGT) generated by two laboratories [using stable isotope-labeled (SIL) peptides or quantitative concatemer (QconCAT)] reflected significant disparity between proteomic methods. Initial analysis of QconCAT data showed lack of correlation with catalytic activity for several UGTs (1A4, 1A6, 1A9, 2B15) and moderate correlations for UGTs 1A1, 1A3, and 2B7 (Rs = 0.40–0.79, $P < 0.05$; $R^2 = 0.30$); good correlations were demonstrated between cytochrome P450 activities and abundances measured in the same experiments. Consequently, a systematic review of data analysis, starting from unprocessed LC-MS/MS data, was undertaken, with the aim of improving accuracy, defined by correlation against activity. Three main criteria were found to be important: choice of monitored peptides and fragments, correction for isotope-label incorporation, and abundance normalization using fractional protein mass. Upon optimization, abundance-activity correlations improved significantly for six UGTs (Rs = 0.53–0.87, $P < 0.01$; $R^2 = 0.48$–0.73); UGT1A9 showed moderate correlation (Rs = 0.47, $P = 0.02$; $R^2 = 0.34$). No spurious abundance-activity relationships were identified. However, methods remained suboptimal for UGT1A3 and UGT1A9; here hydrophobicity of standard peptides is believed to be limiting. This commentary provides a detailed data analysis strategy and indicates, using examples, the significance of systematic data processing following acquisition. The proposed strategy offers significant improvement on existing guidelines applicable to clinically relevant proteins quantified using QconCAT.

Introduction

Robust quantification of proteins involved in drug pharmacokinetics is required for reliable in vitro-in vivo extrapolation of drug-related outcomes (Al Feteisi et al., 2015b). Various quantitative proteomic strategies share several key steps: 1) selection of signature peptides that represent target proteins in biologic samples, with stable isotope-labeled (SIL) versions used as standards, 2) isolation of tissue fractions that contain these proteins, 3) sample preparation for mass spectrometry, by solubilization and proteolysis of proteins into peptides,

and 4) simultaneous analysis of standard and native peptides by liquid chromatography–tandem mass spectrometry (LC-MS/MS) (Wegler et al., 2017). Furthermore, using concatenated standards [quantitative concatemer (QconCAT)] requires additional steps to ensure that standard proteins are successfully expressed and sufficiently labeled, purified, and digested (Russell et al., 2013).

Uridine-5′-diphospho-glucuronosyltransferases (UGTs) have recently attracted more clinical attention (Guillemette et al., 2014), leading to increased interest in UGT abundance and activity data (Margaillan et al., 2015). Our laboratories previously reported comparability of two proteomic assays: in-solution sample preparation with quantification using SIL peptide standards (Fallon et al., 2013) and gel-based sample preparation with QconCAT proteomics (Achour et al., 2014b).

[S] This article has supplemental material available at dmd.aspetjournals.org.

ABBREVIATIONS: BCA, Bicinchoninic acid assay; HLM, human liver microsomes; LC-MS/MS, liquid chromatography–tandem mass spectrometry; MRM, multireaction monitoring; PBPK, physiologically based pharmacokinetics; QconCAT, quantification concatemer; SIL, stable isotope-labeled; UGT, uridine-5′-diphospho-glucuronosyltransferase.

Disparities between abundances generated by these methods pointed to the necessity of validating measurements using UGT-isoform–specific activity. Reliable correlation was demonstrated for the SIL-based measurements; discrepancies remained for the QconCAT-based dataset (Achour et al., 2017b).

The QconCAT methodology has been validated in various contexts (Scott et al., 2016), including, most notably, cytochrome P450 quantification carried out with the UGT measurements (Achour et al., 2014b). Quantification of UGTs led to complications that had not been observed with bacterial (Al-Majdoub et al., 2014) and yeast samples (Brownridge et al., 2011). The proteomic strategy used in this study is inherently complex; however, many steps have been taken to validate

the LC-MS/MS multireaction monitoring (MRM) assay, including assessment of precision and accuracy of measurements, as well as the associated analytical and technical errors (Achour et al., 2014b). Data acquisition constitutes only the first step of data processing, with several subsequent stages aimed at converting these data into abundance levels and then making sense of such levels. These tasks include deciding which elements of the raw data should be used, normalization processes, and quality control checks as applicable. Discrepancies arising at the data analysis stage are not widely appreciated by end-users of proteomic data, especially modelers, and therefore warrant more attention. The aim of this commentary is to highlight the impact of optimizing UGT-specific quantitative factors at the level of data
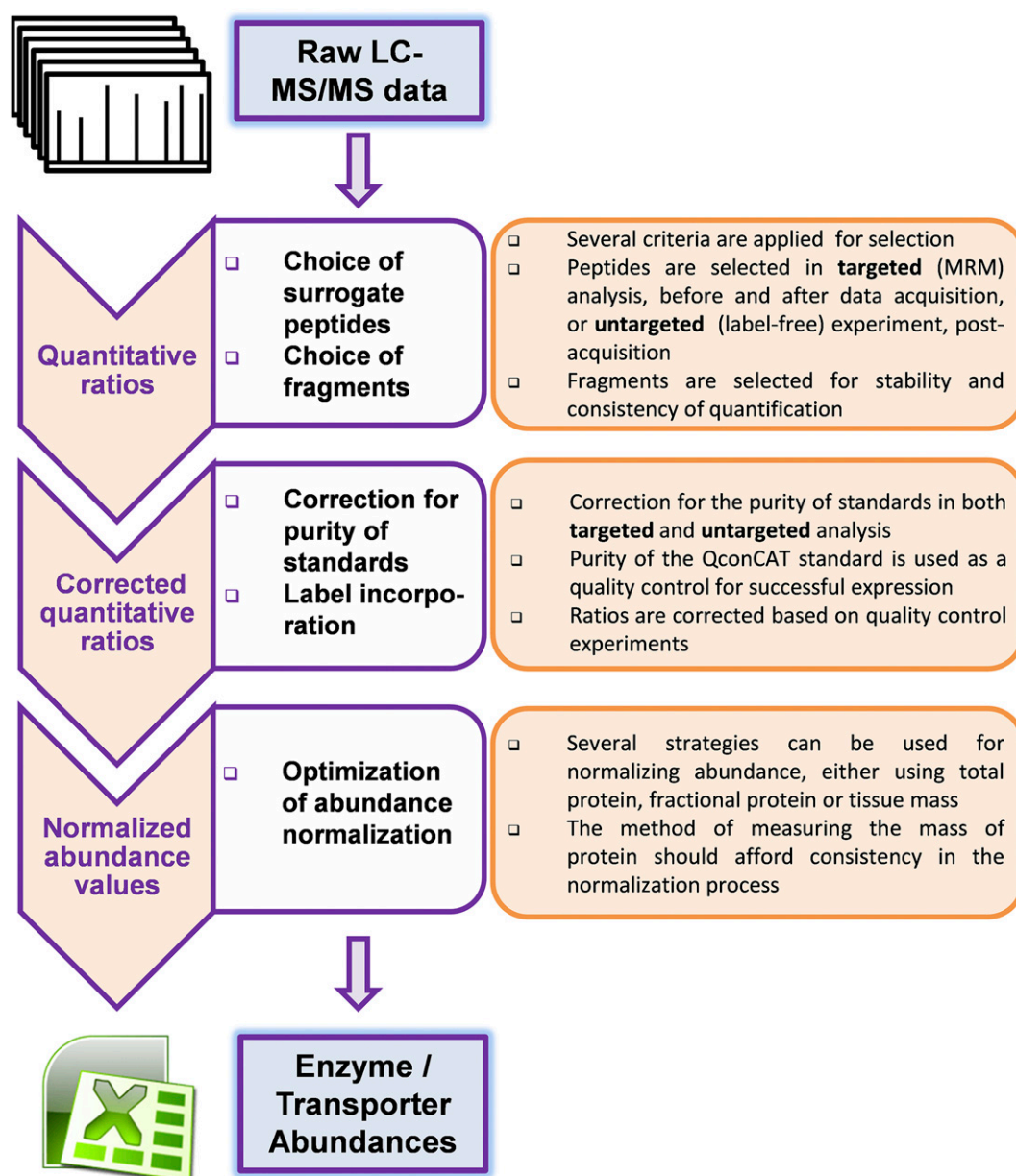

Fig. 1. Schematic of the methodological approach used to assess abundance levels of UGT enzymes using raw LC-MS/MS data. Representative peptides are selected using criteria outlined in Supplemental Methods. This selection process applies to targeted (MRM) and untargeted/global studies. Selection from peptides that are detected consistently in an LC-MS/MS experiment should take into account the uniqueness and the stability of the peptides. Selected fragments should be stable and representative of the peptide (of sufficient length) to return consistent quantification. Correction factors should be applied for label incorporation, especially when low abundance proteins are analyzed. The spike ratio should be consistent with the dynamic range of expression of the target proteins. Normalization should be consistent across all samples and measured parameters. An example of this process is shown in Fig. 2.
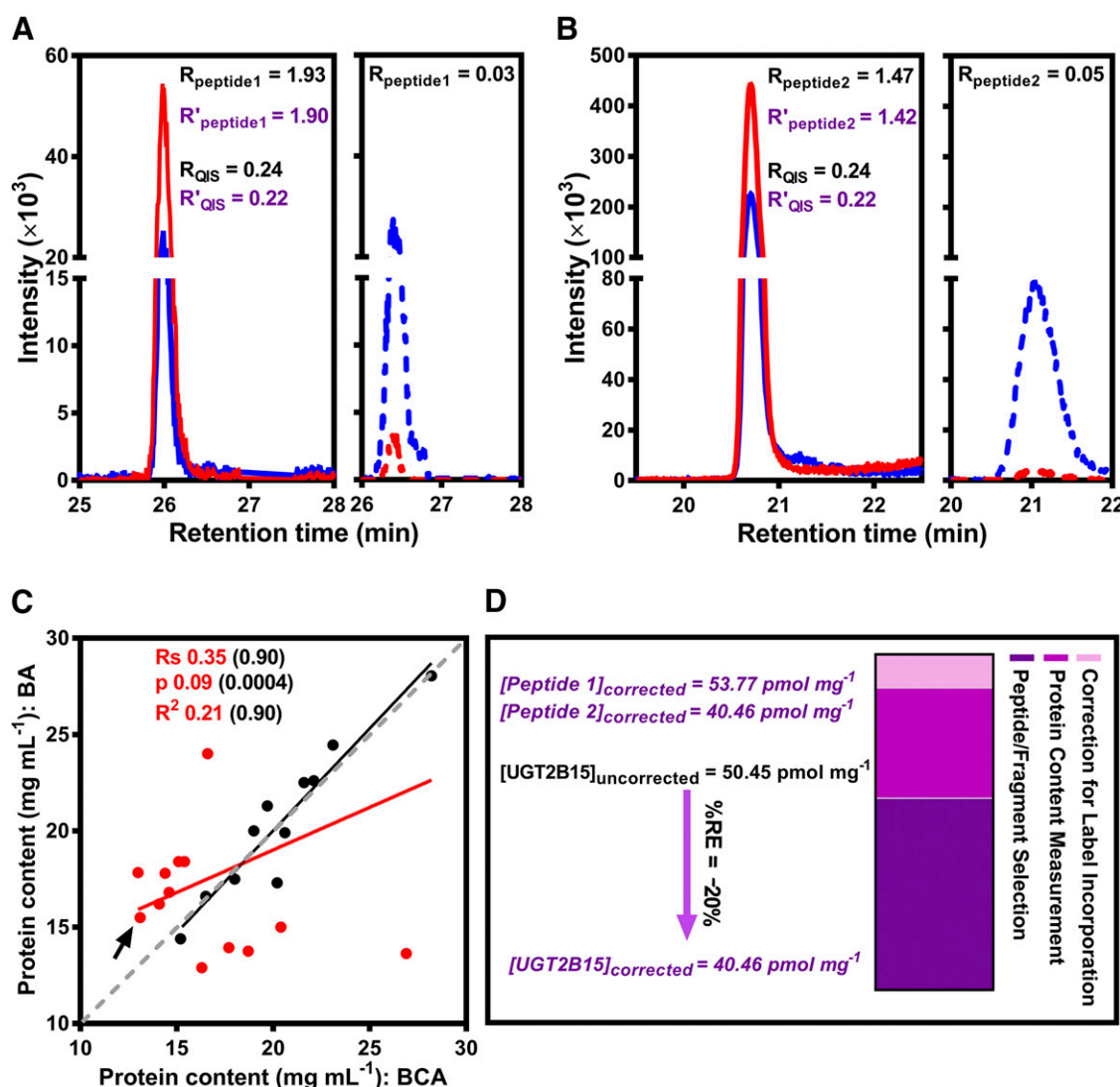
Fig. 2. An example of the assessment process applied to UGT2B15 in sample HH06: choice of peptide standard and correction for label incorporation efficiency (A and B), featuring elution profiles of QconCAT alone (dashed lines), and QconCAT and analyte sample (continuous lines) for heavy (blue) and light (red) peptides (peptide 1: WIYGVSK; peptide 2: SVINDPVYK). Differences between total protein mass measurements using Bradford and BCA assays (C). Calculation of UGT2B15 abundance in sample HH06 using the outlined correction factors and their contributions to the change in reported abundance (D). In (C), the arrow shows sample HH06, and data points in red reflect a difference in content higher than a cut-off relative error (%RE = 100. $(x_{BA,j} - x_{BCA,j})/x_{BCA,j}$) of 15% for each sample j between the two protein content assays. Overall differences in mean and distribution between data from the two assays were nonsignificant according to Mann-Whitney U test; however, individual values were poorly correlated. In (D), the overall shift in abundance was −19.8% (%RE = 100. $(x_{2,i} - x_{1,i})/x_{1,i}$) for enzyme i = UGT2B15 before and after optimization, with the main contributing factor being the selection of peptide/fragment transitions (%RE = −29.8%), followed by total HLM protein content (+18.3%) and correction for label incorporation (+6.1%). Text in purple font reflects corrected values. BA, Bradford assay; QIS, QconCAT-based internal standard.

analysis on QconCAT-measured abundances with reference to catalytic activity.

Reassessment of the Methodological Workflow

Human liver microsomal (HLM) samples ($n = 24$) and methods used to measure UGT abundance and activity were previously described (Achour et al., 2017b). Briefly, eight UGTs (1A1, 1A3, 1A4, 1A6, 1A9, 2B4, 2B7, and 2B15) were independently quantified using QconCAT (Achour et al., 2014b) and SIL-peptide standards (Fallon et al., 2013). Activities of seven enzymes were measured by monitoring the glucuronides of substrates: β-estradiol (UGT1A1), chenodeoxycholic acid (UGT1A3), trifluoperazine (UGT1A4), 5-hydroxytryptophol (UGT1A6), propofol (UGT1A9), zidovudine (UGT2B7), and S-oxazepam (UGT2B15).

Initial QconCAT-based quantification did not show considerable correlation with catalytic activity and therefore required systematic

assessment of several data analysis steps. Figure 1 shows a schematic of the data assessment strategy, with a practical example shown in Fig. 2 (for UGT2B15 in sample HH06). Reanalysis of elution profiles and fragment-based quantitative ratios was done using Skyline 3.7 (Mac-Coss Laboratory Software, Seattle, WA). Measured abundances were reassessed against activity data. An outline of the reassessment strategy is described below.

Choice of Peptide Standards. The peptides that constitute the QconCAT were previously selected on the basis of experimental design followed by theoretical assessment. This approach was limited by options in a data-dependent experiment yielding one to two peptides per UGT (Russell et al., 2013). Extensive sequence homology between UGTs also contributed to this limitation. Initially, peptides that provided higher abundance were used in line with widely accepted literature (Brownridge et al., 2011; Lawless et al., 2016). Instead, we propose

TABLE 1

Assessment of peptides and fragments used to quantify each of the eight UGT enzymes

Protein	Peptide Sequence[a]	In Silico Score (0 to 1)[b]	Theoretical Assessment[c]	Incorporation Correction Factor (%)[d]	MRM Transitions Monitored $[(m/z)^z_{\text{peptide}} \rightarrow (m/z)^z_{\text{fragment}}]$[e]		
UGT1A1	$D_{70}GAFYTLK_{77}$[f]	0.354	++	4.0	$457.73^{+2}/524.31^{+1}$ (y_4)	$457.73^{+2}/671.38^{+1}$ (y_5)	$457.73^{+2}/742.41^{+1}$ (y_6)
	$T_{78}YPVPFQR_{85}$	0.363	++	2.0	$504.27^{2+}/547.30^{+1}$ (y_4)	$504.27^{2+}/646.37^{+1}$ (y_5)	$504.27^{2+}/743.42^{+1}$ (y_6)
UGT1A3	$Y_{164}LSIPTVFFLR_{174}$[f]	0.514	+++	1.0	$678.39^{2+}/681.41^{+1}$ (y_5)	$678.39^{2+}/782.46^{+1}$ (y_6)	$678.39^{2+}/879.51^{+1}$ (y_7)
UGT1A4	$Y_{175}IPCDLDFK_{183}$[f,g]	0.432	+++	5.0	$585.78^{2+}/637.32^{+1}$ (y_5)	$585.78^{2+}/797.35^{+1}$ (y_6)	$585.78^{2+}/894.40^{+1}$ (y_7)
	$G_{184}TQCPNPSSYIPK_{196}$[g]	0.522	+++	5.0	$724.85^{2+}/791.43^{+1}$ (y_7)	$724.85^{2+}/905.47^{+1}$ (y_8)	$724.85^{2+}/1002.53^{+1}$ (y_9)
UGT1A6	$S_{103}FLTAPQTEYR_{113}$[f]	0.554	+++	2.0	$656.83^{2+}/793.38^{+1}$ (y_6)	$656.83^{2+}/864.42^{+1}$ (y_7)	$656.83^{2+}/965.47^{+1}$ (y_8)
	$V_{250}SVWLLR_{256}$[h,i]	0.354	+	1.5	$436.77^{2+}/587.37^{+1}$ (y_4)	$436.77^{2+}/686.43^{+1}$ (y_5)	
UGT1A9	$E_{139}SSFDAVFLDPFDNCGLIVAK_{159}$[f,g]	0.553	++	4.0	$1172.56^{2+}/1233.63^{+1}$ (y_{11})	$1172.56^{2+}/1348.66^{+1}$ (y_{12})	$1172.56^{2+}/1461.74^{+1}$ (y_{13})
	$F_{174}SPGYAIEK_{182}$	0.391	+++	5.0	$506.26^{2+}/623.34^{+1}$ (y_5)	$506.26^{2+}/680.36^{+1}$ (y_6)	$506.26^{2+}/777.41^{+1}$ (y_7)
UGT2B4	$A_{321}NVIASALAK_{330}$[f]	0.412	+++	4.0	$479.29^{2+}/560.34^{+1}$ (y_6)	$479.29^{2+}/673.42^{+1}$ (y_7)	$479.29^{2+}/772.49^{+1}$ (y_8)
UGT2B7	$T_{41}ILDELIQR_{49}$[f]	0.426	++	2.0	$550.82^{2+}/658.39^{+1}$ (y_5)	$550.82^{2+}/773.42^{+1}$ (y_6)	$550.82^{2+}/886.50^{+1}$ (y_7)
	$A_{253}DVWLIR_{259}$[i]	0.300	+	1.5	$436.75^{2+}/587.37^{+1}$ (y_4)	$436.75^{2+}/686.43^{+1}$ (y_5)	$436.75^{2+}/801.46^{+1}$ (y_6)
UGT2B15	$W_{97}IYGVSK_{103}$[h]	0.325	+	3.0	$426.73^{2+}/553.30^{+1}$ (y_5)	$426.73^{2+}/666.38^{+1}$ (y_6)	
	$S_{432}VINDPVYK_{440}$[f]	0.406	++	5.0	$517.78^{2+}/506.30^{+1}$ (y_4)	$517.78^{2+}/735.37^{+1}$ (y_6)	$517.78^{2+}/848.45^{+1}$ (y_7)
MetCAT[j]	$GVNDNEEGFFSAR$[k]	0.561	++++	2.5	$721.32^{2+}/813.39^{+1}$ (y_7)	$721.32^{2+}/942.43^{+1}$ (y_8)	$721.32^{2+}/1056.47^{+1}$ (y_9)

[a] Peptide sequences as defined by the human UniProtKB database (http://www.uniprot.org). Subscript number labels on the C- and N-terminal amino acids of peptide sequences denote their positions in the UGT protein sequences on the basis of their database entries. The terminal lysine (K) and arginine (R) residues were labeled using [$^{13}C_6$] stable isotopes in the QconCAT standard.

[b] In silico assessment was carried out using CONSeQuence algorithm on the basis of charge, hydrophobicity and secondary structure (Eyers et al., 2011).

[c] Theoretical assessment on the basis of criteria outlined in Supplemental Information; arbitrarily, +, ++, +++, and ++++ scores were assigned to peptides under assessment (highest score, ++++) by two independent analysts.

[d] The proportion of light to heavy peptide owing to inefficient incorporation of the ^{13}C label needed to correct quantification ratios; this can be variable from batch to batch.

[e] Up to three transitions for each peptide were designed in silico using Skyline (superscript indicating charge states, z); selected fragments were then appraised on the basis of unique sequences, m/z, quality of elution profiles, and the CV of the returned quantitative ratios. In this table, only the light (native) peptide transitions are listed, where the y-ions (subscript indicates the length of the sequence) were used.

[f] Peptide selected for quantification of each UGT enzyme on the basis of the selection criteria outlined in Supplemental Information and in silico appraisal.

[g] Cysteine residues were alkylated (by carbamidomethylation), necessitating an increment of +57.0215 Da in monoisotopic mass of peptides and certain fragments.

[h] Two transitions were designed and monitored for peptides VSVWLLR (UGT1A6) and WIYGVSK (UGT2B15), which returned low scores on the basis of theoretical, in silico, and fragment assessments. These peptides were excluded from analysis.

[i] The isobaric sequences VSVWLLR (UGT1A6) and ADVWLIR (UGT2B7) were overlapped on the chromatogram owing to close retention times (with the same m/z of parents and fragments). These peptides were excluded from analysis.

[j] MetCAT: QconCAT used as a standard for the quantification of human liver P450 and UGT enzymes (Russell et al., 2013; Achour et al., 2015).

[k] Sequence of QconCAT-based internal standard used for quantification of the QconCAT.

adoption of a better appraisal of quantification that uses as a basis several peptides for each UGT. In this work, assessment of suitability of peptides was carried out on the basis of theoretical appraisal by two independent analysts and in silico evaluation using CONSeQuence algorithm (Eyers et al., 2011). Quantification was subsequently considered on the basis of the more favorable peptide choice (Table 1). Theoretical criteria for peptide assessment are included in Supplemental Methods. Briefly, selected peptides should have unique sequences, and mass-to-charge ratios (of parent and fragment), should not be mapped to membrane-associated domains or subject to polymorphisms or biologic (post-translational) modifications, should be readily cleavable, of suitable length (6–20 amino acids), and have favorable stability (to chemical modification owing to handling/storage) and moderate hydrophobicity (Kamiie et al., 2008; Carroll et al., 2011). Choice of monitored peptide charge state ($z = +2$ or $+3$) was also considered.

Choice of Peptide Fragments. Fragment selection was initially conducted in silico using Skyline 1.4, with fragment ratios expected to return consistent quantification. Initially, two to three transitions per peptide were monitored with mean ratios being used for quantification. In this work, the uniqueness of fragment sequences and consistency between estimates on the basis of monitored transitions were assessed, especially for low abundance proteins; less-specific fragments returning inconsistent ratios were excluded from analysis. In addition, the chromatographic trace of different fragment ions was assessed and poor quality signals were excluded. Since retention time and m/z values monitored had relatively large filters in the LC-MS/MS assay, the m/z values for the selected fragments were assessed, with isobaric and isomeric fragments being excluded (Table 1).

Correction for Efficiency of Label Incorporation. Assessment of efficiency of ^{13}C-label incorporation into QconCAT protein synthesis was previously reported as an in-house quality control step in QconCAT expression; constructs of $\geq 95\%$ purity are accepted as quantitative standards (Achour et al., 2015). The level of incorporation can vary batch-to-batch, and impurity is expected to affect quantification, especially of low abundance proteins (Carr et al., 2014). Uncorrected and corrected quantitative ratios were generated using eqs. 1 and 2, respectively (Fig. 2, A and B):

$$R_{peptide\frac{L}{H}} = \frac{I_{L_{Peptide}}}{I_{H_{QconCAT}}} \qquad (1)$$

$$R'_{peptide\frac{L}{H}} = \frac{I_{L_{Peptide}} - I_{L_{QconCAT}}}{I_{H_{QconCAT}}} \qquad (2)$$

where $R_{peptide\frac{L}{H}}$ and $R'_{peptide\frac{L}{H}}$ are uncorrected and corrected ratios, respectively, used to quantify a peptide representing a UGT enzyme or the QconCAT (using a QconCAT-based internal standard); $I_{L_{Peptide}}$ is the intensity of the light peptide signal measured in the quantitative experiment; $I_{L_{QconCAT}}$ is the peak intensity of the light peptide originating from the QconCAT measured in quality control experiments; and $I_{H_{QconCAT}}$ is the signal intensity of the heavy QconCAT peptide measured in the quantitative experiment.

Normalization of Abundance Measurements. Normalization is commonly applied relative to protein mass, leading to abundance levels expressed in units of picomoles per milligram of fractional protein. Protein mass measurement is normally done by a colorimetric assay, generating data that may not be reproducible. Commonly used assays include: Bradford assay (Bradford, 1976), bicinchoninic acid (BCA) assay (Smith et al., 1985), and tryptophan fluorescence assay (Wiśniewski and Gaugaz, 2015). Abundance and activity were measured by independent laboratories and different protein assays were used (Bradford and BCA assays), demonstrating differences in reported contents for matched samples (Fig. 2C). In this study, a proposed approach to resolving this issue was to normalize abundance and activity

data using protein levels measured by the same assay (BCA assay), using eq. 3.

$$[Enzyme] = [QIS] \cdot \frac{R'_{Peptide_{\frac{L}{H}}}}{R'_{QIS_{\frac{L}{H}}}} \cdot \frac{F_v}{Protein\ Mass} \qquad (3)$$

where $[Enzyme]$ is target enzyme abundance (expressed in picomoles per milligram of HLM protein); $[QIS]$ represents the concentration of the unlabeled internal standard used to quantify the QconCAT [a Glu^1-fibrinopeptide B analog, modified to reduce the incidence of missed cleavage owing to the glutamate at the N-terminus (Lawless and Hubbard, 2012)]; F_v is a volume correction factor relating the analyzed volume to the volume of HLM sample; and Protein Mass is the protein content determined for each sample (BCA assay). The terms assessed in this report were: target peptide and QconCAT-based–internal-standard ratios (parent-fragment selection and correction for label incorporation) and protein mass used for normalization (Fig. 2D).

Statistical Assessment of the Optimization Process. Correlations were assessed at each stage using Spearman correlation test (Rs) and scatter of data was assessed with linear regression (R^2). The following criteria were used: α-value of 0.05 (Bonferroni-corrected for correlation matrices), strong correlation ($Rs > 0.50$) and limited scatter ($R^2 > 0.30$), taking into account the effect of abundance/activity units, as previously advocated (Achour et al., 2017a).

Effects of Systematic Appraisal on Endpoint Measurements

To generate reliable proteomic data for in vitro-in vivo extrapolation–physiologically based pharmacokinetics, best practice must be ensured throughout the entire quantitative workflow, including data processing. It is important to note that sample preparation and LC-MS/MS methods have previously undergone quality evaluation and returned precise and accurate quantification of cytochromes P450 in relation to genotype and activity (Achour et al., 2014b). Therefore, only factors specifically affecting UGT measurements were considered.

Effects of the Choice of Monitored Peptides/Fragments. Mass spectrometry-based proteomic strategies rely on using peptides as surrogates for proteins, and the limitations of this approach are still being uncovered. In eukaryotes, protein truncation and splice variants can result in misleading measurements, and technical issues include signal overlap and variable peptide responses between runs. QconCAT design normally follows a pragmatic approach, with two or more peptides included for each protein (Pratt et al., 2006); however, only one peptide is ultimately used for quantification. Two peptides representing each UGT were therefore included in the QconCAT whenever possible. Table 1 shows sequences used in data acquisition, scored on the basis of theoretical and in silico criteria; Supplemental Fig. 1 shows peptide elution profiles. Theoretical assessment of peptide suitability involves consideration of several parameters, which tend to be prioritized somewhat subjectively, and was therefore conducted by two independent analysts; the analysts' scores were in agreement and compared well with in silico assessment. Three pairs of peptides (representing UGTs 1A1, 1A4, and 2B7) returned consistent quantification (Supplemental Fig. 2), whereas three pairs (UGTs 1A6, 2B4, and 2B15) showed significant differences.

When two or more peptides are used to quantify a protein, preference has conventionally been given to peptides that return higher concentrations (Brownridge et al., 2011; Lawless et al., 2016); the assumption is that underestimation can occur owing to differences in efficiency of release of peptides. It has recently become clear that several peptide-related factors can affect measurements and should therefore be considered when peptide choice is made, ideally in the design stage, although this is not always possible, especially in global proteomics. The
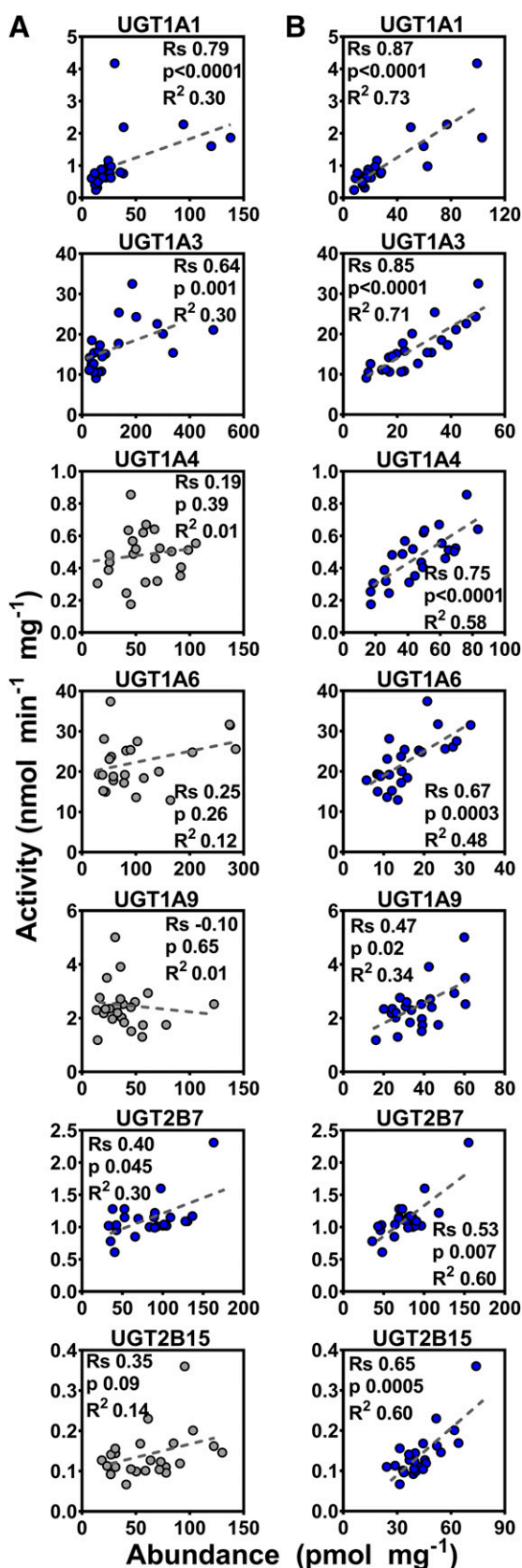
Fig. 3. Correlation between individual UGT enzyme abundances and activity rates ($n = 24$) using the original dataset (A) and the reassessed data on the basis of the proposed strategy (B). Moderate to strong, statistically significant correlations are shown in blue and weak correlations in gray. Units of abundance-measurement are picomoles per milligram of HLM protein, and units of catalytic activity are nanomoles (glucuronide) per minute per milligram of HLM protein. Substrates used for activity measurement are: β-estradiol (UGT1A1), chenodeoxycholic acid (UGT1A3), trifluoperazine (UGT1A4), 5-hydroxytryptophol (UGT1A6), propofol (UGT1A9), zidovudine (UGT2B7), S-oxazepam (UGT2B15). Rs, Spearman correlation coefficient. Dashed lines represent lines of regression.

strategy of monitoring the "highest reporter" will probably work well when soluble proteins are quantified; however, for membrane-bound proteins, especially those with unknown structures (e.g., UGTs), a more secure strategy is to monitor "best performer" peptides. Discerning best performers will almost always involve visual examination of MS and MS/MS spectra. For example, isobaric sequences representing UGT1A6 (WIYGVSK) and UGT2B7 (ADVWLIR) overlapped on the chromatogram, leading to overestimation of abundance, especially for UGT1A6. Discrepancies in abundance in relation to peptide choice have previously been reported to reach up to 30-fold in the case of P-glycoprotein in hepatocytes (Chen et al., 2017), and therefore applying suitable criteria is essential to ensure quality of surrogate peptides (Bhatt and Prasad, 2018). Such criteria were previously used in a label-free experiment on matched liver samples, which resulted in good agreement with QconCAT measurements of several UGT enzymes (Achour et al., 2017a).

Because targeted quantification uses MS/MS data as a basis, the properties of fragments are as important as those of parent peptides. Carr et al. (2014) recommended monitoring three to five fragments, allowing inconsistencies in measurements to be reconciled. Fragments are typically selected in silico on the basis of predicted peak intensities rather than sequence properties (Carr et al., 2014). There are several potential pitfalls with this approach. First, MS/MS spectra may have several low intensity peaks (especially with proline-containing peptides), so that a lower number of consistent measurements can be made. Two peptides, YLSIPTVFFLR (UGT1A3) and ESSFDAVFLDPFDNC-GLIVAK (UGT1A9), were subject to this error, when peaks of lower quality returned inconsistent ratios. Although optimizing transition selection resulted in improved correlation with activity, quantitative methods for these two enzymes still require improvement. Additionally, erroneous quantification can occur when uniqueness of peptide-to-fragment m/z values cannot be ensured, most often in complex biologic mixtures, with short sequences being most affected (Carr et al., 2014). The MRM filters (retention time, parent ion m/z, and fragment ion m/z) are normally sufficient to ensure exclusive selection of fragments, but not always, especially in nonscheduled experiments, where retention times are not specified. Peptide sequences WIYGVSK (UGT1A6), ADVWLIR (UGT2B7), and WIYGVSK (UGT2B15) were eventually excluded from analysis for isobaric interference despite returning levels higher than their alternatives. The combined effect of peptide and fragment selection was shown to be substantial (Supplemental Table 1), with abundance values changing 0.5-to 3-fold upon reassessment. This led to improved abundance-activity correlation for most UGT enzymes. The initially weak correlation for UGTs 1A4, 1A6, and 2B15 ($Rs = 0.19$–0.35, $P > 0.05$; $R^2 = 0.01$–0.14) became moderate ($Rs = 0.52$–0.56, $P < 0.01$; $R^2 = 0.24$–0.31). For other UGTs (1A1, 1A3, 2B7), this improved mainly in terms of data scatter (from $R^2 = 0.30$ to $R^2 = 0.47$–0.57), although correlation for UGT1A9 remained weak ($Rs = 0.20$, $P = 0.33$, $R^2 = 0.07$).

Effects of Correction for the Quality of Isotopically Labeled Standards. QconCATs are artificial proteins expressed in-house, and the extent of labeling varies, depending on the construct and culture conditions, from ∼95–99% (Achour et al., 2015). This means that QconCATs can contribute unlabeled peptide that may affect quantification when the analyte is expressed at low levels (Carr et al., 2014). Table 1 shows the extent of label incorporation into each peptide, reflecting more efficient labeling of arginines than lysines (Russell et al.,
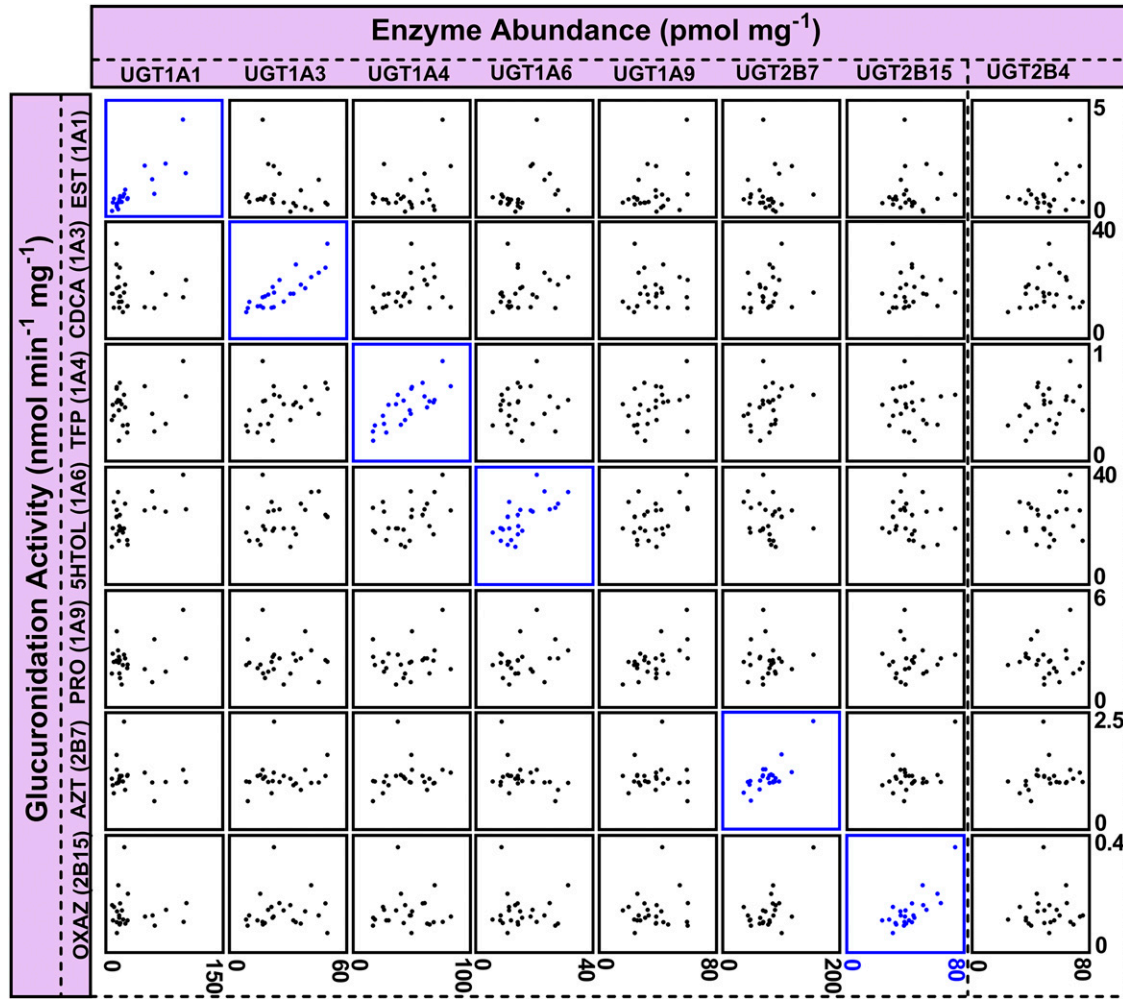
Fig. 4. Correlation matrix of QconCAT-derived individual UGT enzyme abundances ($n = 24$) and activity rates (abundance vs. activity). Strong, statistically significant correlations are shown in blue. Units of abundance-measurement are picomoles per milligram of HLM protein, and units of catalytic activity are nanomoles (glucuronide) per minute per milligram of HLM protein. AZT, zidovudine; CDCA, chenodeoxycholic acid; EST, β-estradiol; 5HTOL, 5-hydroxytryptophol; OXAZ, S-oxazepam; PRO, propofol; TFP, trifluoperazine. Supplemental Table 2 shows the statistical analysis used to generate the abundance-activity correlation matrix.

2013). The outcome of correction for purity was that levels of UGTs had a variable artifactual component of up to 10%, with little effect on correlation with activity. A similar trend was observed with efflux transporters BCRP and MRP2, quantified in human jejunum using QconCAT methodology (Harwood et al., 2015), which were overestimated on average by 10% and 7%, respectively, when corrections for purity were not considered (Harwood et al., 2016a). However, these errors do not always lead to meaningful differences in pharmacokinetic outcomes (Harwood et al., 2016b).

Effects of Normalization of Abundances. Normalization relies on protein content determination using colorimetric assays, which are prone to interference from reagents commonly used in routine sample processing, including detergents, chaotropes, and reducing agents (Wiśniewski and Gaugaz, 2015). In particular, BCA assay is incompatible with commonly used concentrations of urea and dithiothreitol (Smith et al., 1985), whereas Bradford reagent tends to interact with sodium dodecyl sulfate (Bradford, 1976), a detergent used for gel-based sample preparation. A limitation of the cross-laboratory study (Achour et al., 2017b) was the use of Bradford assay with QconCAT measurements, whereas both activity and SIL-based measurements were normalized using BCA assay. Comparing the two protein measurements (Fig. 2C) indicates that, although average protein content in the samples was

similar, there was no correlation between individual values. Normalization against the same protein content resulted in changes in enzyme levels reaching up to 50%, with improved correlation with activity, mainly in terms of scatter for six UGTs (from $R^2 = 0.24$–0.57 to $R^2 = 0.48$–0.73), and UGT1A9 showed substantial improvement to moderate correlation ($Rs = 0.47$, $P = 0.02$; $R^2 = 0.34$). It is not clear, however, whether BCA-normalization leads to better results; it may just lead to more consistent error. We have recently illustrated that normalization relative to tissue mass instead of fractional protein introduces less artifactual variability to end-point measurements (Achour et al., 2017a).

Overall Effects of Systematic Reassessment on UGT Measurements. Specific effects of the assessed factors on abundance of each enzyme are described in Supplemental Results. Collectively, the proposed strategy led to 0.5- to 3.3-fold change in UGT levels, with substantial improvement in correlation with activity (Fig. 3) and tighter levels of interindividual variability in abundance (26%–86%), matching variability in activity (27%–67%), in line with recent literature (Margaillan et al., 2015). In addition, cross-laboratory comparison of UGT abundances seemed to indicate overall agreement, returning generally interchangeable abundance values (Supplemental Figs. 3 and 4). On the basis of these considerations, a list of established UGT-specific methods was generated (Supplemental Table 4).

The correlation matrix (Fig. 4) confirms specificity of protein and activity data, with no evidence of spurious abundance-activity relationships. A similar complementary approach was used previously to discern tissue-specific glycolytic and gluconeogenic pathways (Wiśniewski et al., 2015). Expression intercorrelations uncovered in the UGT dataset (Supplemental Table 3) were also in line with literature (Achour et al., 2014a; Margaillan et al., 2015). Correlations of enzyme expression have recently been adopted for more realistic model-based predictions of drug clearance and drug-drug interactions (Barter et al., 2010; Doki et al., 2018), with additional established correlations making their way into commonly used platforms, such as Simcyp.

Conclusions. The QconCAT approach offers several advantages (Al Feteisi et al., 2015a), and therefore it has recently been adopted for various clinical and biologic applications (Dzieciatkowska et al., 2015; Wang et al., 2015; Kito et al., 2016). Although initial applications were primarily aimed to quantify soluble proteins, often in simple organisms, it is clear that QconCAT can be applied to membrane-bound mammalian proteins. However, monitored peptides and fragments need to be chosen carefully, preferably using a priori selection, and corrections are required for relatively low purity standard peptides targeted at low abundance proteins. We continue to advocate using tissue mass for abundance normalization and activity data for quality control. We propose optimized QconCAT methods for the quantification of several UGTs (1A1, 1A6, 2B4, 2B7, and 2B15) and a robust data analysis strategy for targeted proteomic quantification, particularly applicable for QconCAT-based measurements.

Acknowledgments

Authorship Contributions

Participated in research design: Achour, Dantonio, Niosi, Novak, Al-Majdoub, Goosen, Rostami-Hodjegan, Barber.

Performed data analysis: Achour, Dantonio, Niosi, Novak, Al-Majdoub.

Wrote or contributed to the writing of the manuscript: Achour, Dantonio, Niosi, Novak, Al-Majdoub, Goosen, Rostami-Hodjegan, Barber.

References

Achour B, Al Feteisi H, Lanucara F, Rostami-Hodjegan A, and Barber J (2017a) Global proteomic analysis of human liver microsomes: rapid characterization and quantification of hepatic drug-metabolizing enzymes. *Drug Metab Dispos* **45**:666–675.

Achour B, Al-Majdoub ZM, Al Feteisi H, Elmorsi Y, Rostami-Hodjegan A, and Barber J (2015) Ten years of QconCATs: application of multiplexed quantification to small medically relevant proteomes. *Int J Mass Spectrom* **391**:93–104.

Achour B, Dantonio A, Niosi M, Novak JJ, Fallon JK, Barber J, Smith PC, Rostami-Hodjegan A, and Goosen TC (2017b) Quantitative characterization of major hepatic UDP-glucuronosyltransferase enzymes in human liver microsomes: comparison of two proteomic methods and correlation with catalytic activity. *Drug Metab Dispos* **45**:1102–1112.

Achour B, Rostami-Hodjegan A, and Barber J (2014a) Protein expression of various hepatic uridine 5′-diphosphate glucuronosyltransferase (UGT) enzymes and their inter-correlations: a meta-analysis. *Biopharm Drug Dispos* **35**:353–361.

Achour B, Russell MR, Barber J, and Rostami-Hodjegan A (2014b) Simultaneous quantification of the abundance of several cytochrome P450 and uridine 5′-diphospho-glucuronosyltransferase enzymes in human liver microsomes using multiplexed targeted proteomics. *Drug Metab Dispos* **42**:500–510.

Al Feteisi H, Achour B, Barber J, and Rostami-Hodjegan A (2015a) Choice of LC-MS methods for the absolute quantification of drug-metabolizing enzymes and transporters in human tissue: a comparative cost analysis. *AAPS J* **17**:438–446.

Al Feteisi H, Achour B, Rostami-Hodjegan A, and Barber J (2015b) Translational value of liquid chromatography coupled with tandem mass spectrometry-based quantitative proteomics for in vitro-in vivo extrapolation of drug metabolism and transport and considerations in selecting appropriate techniques. *Expert Opin Drug Metab Toxicol* **11**:1357–1369.

Al-Majdoub ZM, Carroll KM, Gaskell SJ, and Barber J (2014) Quantification of the proteins of the bacterial ribosome using QconCAT technology. *J Proteome Res* **13**:1211–1222.

Barter ZE, Perrett HF, Yeo KR, Allorge D, Lennard MS, and Rostami-Hodjegan A (2010) Determination of a quantitative relationship between hepatic CYP3A5*1/*3 and CYP3A4 expression for use in the prediction of metabolic clearance in virtual populations. *Biopharm Drug Dispos* **31**:516–532.

Bhatt DK and Prasad B (2018) Critical issues and optimized practices in quantification of protein abundance level to determine interindividual variability in DMET proteins by LC-MS/MS proteomics. *Clin Pharmacol Ther* **103**:619–630.

Bradford MM (1976) A rapid and sensitive method for the quantitation of microgram quantities of protein utilizing the principle of protein-dye binding. *Anal Biochem* **72**:248–254.

Brownridge P, Holman SW, Gaskell SJ, Grant CM, Harman VM, Hubbard SJ, Lanthaler K, Lawless C, O'Cualain R, Sims P, et al. (2011) Global absolute quantification of a proteome: challenges in the deployment of a QconCAT strategy. *Proteomics* **11**:2957–2970.

Carr SA, Abbatiello SE, Ackermann BL, Borchers C, Domon B, Deutsch EW, Grant RP, Hoofnagle AN, Hüttenhain R, Koomen JM, et al. (2014) Targeted peptide measurements in biology and medicine: best practices for mass spectrometry-based assay development using a fit-for-purpose approach. *Mol Cell Proteomics* **13**:907–917.

Carroll KM, Simpson DM, Eyers CE, Knight CG, Brownridge P, Dunn WB, Winder CL, Lanthaler K, Pir P, Malys N, et al. (2011) Absolute quantification of the glycolytic pathway in yeast: deployment of a complete QconCAT approach. *Mol Cell Proteomics* **10**:M111. 007633.

Chen B, Liu L, Ho H, Chen Y, Yang Z, Liang X, Payandeh J, Dean B, Hop CECA, and Deng Y (2017) Strategies of drug transporter quantitation by LC-MS: importance of peptide selection and digestion efficiency. *AAPS J* **19**:1469–1478.

Doki K, Darwich AS, Achour B, Tornio A, Backman JT, and Rostami-Hodjegan A (2018) Implications of intercorrelation between hepatic CYP3A4-CYP2C8 enzymes for the evaluation of drug-drug interactions: a case study with repaglinide. *Br J Clin Pharmacol* DOI: 10.1111/bcp.13533 [published ahead of print].

Dzieciatkowska M, D'Alessandro A, Hill RC, and Hansen KC (2015) Plasma QconCATs reveal a gender-specific proteomic signature in apheresis platelet plasma supernatants. *J Proteomics* **120**:1–6.

Eyers CE, Lawless C, Wedge DC, Lau KW, Gaskell SJ, and Hubbard SJ (2011) CONSeQuence: prediction of reference peptides for absolute quantitative proteomics using consensus machine learning approaches. *Mol Cell Proteomics* **10**:M110.003384.

Fallon JK, Neubert H, Hyland R, Goosen TC, and Smith PC (2013) Targeted quantitative proteomics for the analysis of 14 UGT1As and -2Bs in human liver using NanoUPLC-MS/MS with selected reaction monitoring. *J Proteome Res* **12**:4402–4413.

Guillemette C, Lévesque É, and Rouleau M (2014) Pharmacogenomics of human uridine diphospho-glucuronosyltransferases and clinical implications. *Clin Pharmacol Ther* **96**:324–339.

Harwood MD, Achour B, Neuhoff S, Russell MR, Carlson G, Warhurst G, and Rostami-Hodjegan A (2016a) In vitro–in vivo extrapolation scaling factors for intestinal P-glycoprotein and breast cancer resistance protein: part I: a cross-laboratory comparison of transporter-protein abundances and relative expression factors in human intestine and Caco-2 cells. *Drug Metab Dispos* **44**:297–307.

Harwood MD, Achour B, Neuhoff S, Russell MR, Carlson G, Warhurst G, and Rostami-Hodjegan A (2016b) In vitro–in vivo extrapolation scaling factors for intestinal P-glycoprotein and breast cancer resistance protein: part II. The impact of cross-laboratory variations of intestinal transporter relative expression factors on predicted drug disposition. *Drug Metab Dispos* **44**:476–480.

Harwood MD, Achour B, Russell MR, Carlson GL, Warhurst G, and Rostami-Hodjegan A (2015) Application of an LC-MS/MS method for the simultaneous quantification of human intestinal transporter proteins absolute abundance using a QconCAT technique. *J Pharm Biomed Anal* **110**:27–33.

Kamiie J, Ohtsuki S, Iwase R, Ohmine K, Katsukura Y, Yanai K, Sekine Y, Uchida Y, Ito S, and Terasaki T (2008) Quantitative atlas of membrane transporter proteins: development and application of a highly sensitive simultaneous LC-MS/MS method combined with novel in-silico peptide selection criteria. *Pharm Res* **25**:1469–1483.

Kito K, Okada M, Ishibashi Y, Okada S, and Ito T (2016) A strategy for absolute proteome quantification with mass spectrometry by hierarchical use of peptide-concatenated standards. *Proteomics* **16**:1457–1473.

Lawless C, Holman SW, Brownridge P, Lanthaler K, Harman VM, Watkins R, Hammond DE, Miller RL, Sims PF, Grant CM, et al. (2016) Direct and absolute quantification of over 1800 yeast proteins via selected reaction monitoring. *Mol Cell Proteomics* **15**:1309–1322.

Lawless C and Hubbard SJ (2012) Prediction of missed proteolytic cleavages for the selection of surrogate peptides for quantitative proteomics. *OMICS* **16**:449–456.

Margaillan G, Rouleau M, Klein K, Fallon JK, Caron P, Villeneuve L, Smith PC, Zanger UM, and Guillemette C (2015) Multiplexed targeted quantitative proteomics predicts hepatic glucuronidation potential. *Drug Metab Dispos* **43**:1331–1335.

Pratt JM, Simpson DM, Doherty MK, Rivers J, Gaskell SJ, and Beynon RJ (2006) Multiplexed absolute quantification for proteomics using concatenated signature peptides encoded by QconCAT genes. *Nat Protoc* **1**:1029–1043.

Russell MR, Achour B, Mckenzie EA, Lopez R, Harwood MD, Rostami-Hodjegan A, and Barber J (2013) Alternative fusion protein strategies to express recalcitrant QconCAT proteins for quantitative proteomics of human drug metabolizing enzymes and transporters. *J Proteome Res* **12**:5934–5942.

Scott KB, Turko IV, and Phinney KW (2016) QconCAT: internal standard for protein quantification. *Methods Enzymol* **566**:289–303.

Smith PK, Krohn RI, Hermanson GT, Mallia AK, Gartner FH, Provenzano MD, Fujimoto EK, Goeke NM, Olson BJ, and Klenk DC (1985) Measurement of protein using bicinchoninic acid. *Anal Biochem* **150**:76–85.

Wang H, Zhang H, Li J, Wei J, Zhai R, Peng B, Qiao H, Zhang Y, and Qian X (2015) A new calibration curve calculation method for absolute quantification of drug metabolizing enzymes in human liver microsomes by stable isotope dilution mass spectrometry. *Anal Methods* **7**:5934–5941.

Wegler C, Gaugaz FZ, Andersson TB, Wiśniewski JR, Busch D, Gröer C, Oswald S, Norén A, Weiss F, Hammer HS, et al. (2017) Variability in mass spectrometry-based quantification of clinically relevant drug transporters and drug metabolizing enzymes. *Mol Pharm* **14**:3142–3151.

Wiśniewski JR and Gaugaz FZ (2015) Fast and sensitive total protein and peptide assays for proteomic analysis. *Anal Chem* **87**:4110–4116.

Wiśniewski JR, Gizak A, and Rakus D (2015) Integrating proteomics and enzyme kinetics reveals tissue-specific types of the glycolytic and gluconeogenic pathways. *J Proteome Res* **14**:3263–3273.

Address correspondence to: Dr. Jill Barber, Centre for Applied Pharmacokinetic Research, Division of Pharmacy and Optometry, School of Health Sciences, University of Manchester, Stopford Building, Oxford Road, Manchester, M13 9PT, United Kingdom. E-mail: Jill.Barber@manchester.ac.uk

Data Generated by Quantitative LC-MS Proteomics Are Only the Start and Not the Endpoint: Optimization of QconCAT-Based Measurement of Hepatic UDP-Glucuronosyltransferase Enzymes with Reference to Catalytic Activity

Brahim Achour, Alyssa Dantonio, Mark Niosi, Jonathan J. Novak, Zubida M Al-Majdoub,

Theunis C. Goosen, Amin Rostami-Hodjegan, and Jill Barber

Brahim Achour, Alyssa Dantonio, Mark Niosi, Jonathan J. Novak, Zubida M Al-Majdoub, Theunis C. Goosen, Amin Rostami-Hodjegan and Jill Barber

1. Supplemental Methods

1.1 Theoretical and *in silico* peptide and fragment selection

Initially, the design of the MetCAT construct was supported primarily by experimental data. Theoretically, the selection criteria (Pratt et al., 2006; Kamiie et al., 2008; Achour et al., 2015) normally used in the design of peptide standards include:

A. Primary selection criteria

1. **Proteotypic peptide sequence**, unique against the target proteome to ensure exclusive quantification of target protein.

2. **Cleavable sequence** by the selected proteolytic enzymes, normally with C-terminal arginine and lysine, not followed closely by proline (KP, RP), for trypsin and lysyl-endoproteinase enzymes.

3. **Unique m/z values for the peptide and and its fragments** to avoid overlapping peaks (isobaric and isomeric analytes), for example peptides with leucine (L) and isoleucine (I) have the same *m/z* values for parent and fragment ions.

4. **Avoiding peptides in transmembrane regions** for efficient solubilization and subsequent cleavage by proteolytic enzymes.

5. **Optimal sequence length** (6-20) to facilitate elution using HPLC and compatibility with different mass spectrometric platforms.

6. **Avoiding confirmed polymorphic (SNV) and post-translationally modified (PTM) sites as well as splice variants** which can lead to false quantification (except if stoichiometric assessment is targeted in the study).

7. **Avoiding highly unstable sites** including reactive amino acids (especially M), deamindation prone sites (especially NG) and non-enzymatic hydrolysis prone motifs (especially DP under acidic conditions). These are artefacts of sample processing and storage that can affect analyte and standard peptides differently, leading to errors in quantification (Carroll et al., 2011).

B. Secondary selection criteria

1. **Avoiding unstable sites** (additional to point 7 above) including other reactive amino acids (W, H), deamindation prone sites (QG, NQ) and non-enzymatic hydrolysis prone motifs (NP). Highly reactive sites that can be modified (C) should be avoided whenever possible.

2. **Avoiding missed cleavage-prone sequences** including proximity of cleavage sites (on both termini) to acidic residues (D, E) and di/tri-basic contexts at the cleavage site, called ragged ends (KK, KR, RK, RR). Proximity is defined as within 3 amino acid positions of the cleavage site.

3. **Optimal hydrophobicity** to select peptides sufficiently soluble in solution, which can readily be eluted from the HPLC column, and to elicit a good quality elution profile. In addition, overlap between elution profiles can complicate the quantification process.

4. **Consistent observation using LC-MS** in the analysed biological matrix. Because not all peptides are consistently observed under mass spectrometric conditions (Kuster et al., 2005), it is desirable that the selected peptide should be consistently quantifiable using the selected LC-MS platform in its native biological matrix (Mallick et al., 2007).

5. **Avoiding peptide sequences proximal to the C- and N-terminus** in native proteins, which tend to be subject to endogenous proteolytic degradation.

6. **Long fragment ions** preferably of higher *m/z* than the parent ion to ensure uniqueness of the selected transition towards the rest of the proteome.

In addition to theoretical criteria, *in silico* assessment was also carried out using CONSeQuence (Eyers et al., 2011), to assess peptide behaviour under MS conditions based on mainly peptide charge properties, hydrophobicity and structure, and Phobius (Käll et al., 2007), to predict UGT transmembrane domains and peptides that should be avoided. The PeptideAtlas (Deutsch, 2010) database was also used to search the most suitable UGT peptides and assess fragmentation properties, and the GPM database (Fenyö et al., 2010) to assess the monitored fragments for suitable transitions in MRM experiments.

1.2 Additional statistical data analysis

Normality of distribution in the activity and abundance values was assessed using D'Agostino-Pearson, Shapiro-Wilk and Kolmogorov-Smirnov tests. Non-parametric statistical assessment was selected due to lack of normality (non-Gaussian distribution) in most datasets (both abundance and activity data). Assessment of differences between datasets was carried out using Mann-Whitney *U*-test, and discrepancies in distribution were assessed with Kolmogorov-Smirnov cumulative distribution test. Outlier identification was carried out using iterative Grubbs' test.

Fold differences were assessed using average fold error ($AFE = 10^{\left[\frac{\sum_1^n \text{Log}\left(x_{QconCAT,i}/x_{SIL,i}\right)}{n}\right]}$) and absolute average fold error ($AAFE = 10^{\left[\frac{\sum_1^n |\text{Log}\left(x_{QconCAT,i}/x_{SIL,i}\right)|}{n}\right]}$), for the abundance of each enzyme *i*, to assess bias and scatter of data, measured using the two proteomic methods as reported previously (Fallon et al., 2013; Achour et al., 2014). AFE and AAFE were also used to assess differences in QconCAT-derived data before and after optimization of analysis.

Data Generated by Quantitative LC-MS Proteomics Are Only the Start and Not the Endpoint: Optimization of QconCAT-Based Measurement of Hepatic UDP-Glucuronosyltransferase Enzymes with Reference to Catalytic Activity

Brahim Achour, Alyssa Dantonio, Mark Niosi, Jonathan J. Novak, Zubida M Al-Majdoub, Theunis C. Goosen, Amin Rostami-Hodjegan and Jill Barber

Correlations between abundance-activity datasets were assessed using Spearman rank order correlation coefficient ($R_s = 1 - \frac{6 \sum_1^n \left(Rank_{y_{2,i}} - Rank_{x_{1,i}} \right)^2}{n \left(n^2 - 1 \right)}$) for each enzyme i characterized using method 1 (x: abundance) and method 2 (y: activity), with n representing the number of samples (n=24). The scatter was measured using correlation coefficient (R^2) based on linear regression analysis. To generate the matrices, the level of significance of the p-value was adjusted in relation to the number of iterative tests using a Bonferroni correction ($\alpha' = 1 - (1 - \alpha)^{1/k}$), where α' is the corrected significance level, α is the uncorrected significance level nominally set at 0.05 and k is the number of iterations (k=7, for abundance-activity and abundance-abundance matrices). The corrected significance level was therefore set at α'=0.01, rounded up to two decimal places. Microsoft Excel 2010 and GraphPad® Prism version 7.03 (GraphPad Software, San Diego, CA) were used for statistical analysis and illustrations.

2. Supplemental Results

2.1 Optimization of QconCAT data analysis

Table 1 in the manuscript shows the peptide sequences selected for quantitative analysis, with theoretical and *in silico* scores assigned to each peptide. Appraisal of sequence pairs for each UGT enzyme is included below. **Supplemental Table 1** shows the effects of optimization on abundance measurements of UGT enzymes using the optimized data analysis strategy, with effects on correlation between activity and abundance data shown in **Figure 3**. **Supplemental Figure 1** shows the elution profiles of the peptides used in this experiment. Assessment of correlation between abundance measurements using the two QconCAT peptides representing each UGT enzyme after optimization is shown in **Supplemental Figure 2**. Although peptides showed reasonable correlation, the scale of abundance levels reflected large disparity between peptide pairs (especially for UGT1A6), with the less favorable surrogates showing a higher number of outliers. The presence of these outliers tended to ultimately affect the quality of abundance-activity correlation.

UGT1A1. The peptide selection TYPVPFQR is not favorable due to potential missed cleavage due to the presence of a dibasic context at the cleavage site (RK), as well as proximity to glutamic (E) and aspartic (D) acid residues (TYPVPFQR.KED), both factors known to disrupt digestion efficiency (Lawless and Hubbard, 2012). This was less the case for the other signature peptide (R.DGAFYTLK.T). In addition, while the peptide DGAFYTLK is predicted to be water-soluble, the sequence TYPVPFQR consists of several hydrophobic amino acids (P, V, P, F), which make this peptide poorly soluble in aqueous solutions. The

presence of two proline (P) residues in its sequence is predicted to cause non-favourable fragmentation due to the presence of dominant fragments.

UGT1A4. The peptide selection GTQCPNPSSYIPK is not expected to provide reliable quantitative data over YIPCDLDFK for several reasons, including the proximity of the cleavage site to an acidic residue (DFK.GTQCPNPSSYIPK) and the presence of NP bond leading to spontaneous non-enzymatic cleavage, especially under acidic conditions (formic acid pH ~3.0). Structural properties also indicate unfavorable fragmentation due the presence of three proline residues along its sequence. Both peptide sequences contain the highly reactive residue cysteine (C), which is efficiently blocked upon carbamidomethylation prior to digestion.

UGT1A6. The peptide sequence VSVWLLR is expected to return erroneous quantitative ratios due to its high hydrophobicity (V, V, W, L, L), leading to poor solubility; instability due to the presence of tryptophan (W); predicted poor detectability under LC-MS conditions and small number of predicted transitions. This peptide has an isobaric sequence to ADVWLIR (UGT2B7). Susceptibility to missed cleavage is expected for both peptide surrogates due to proximity of cleavage sites to an aspartate (VSVWLLR.YD) and a glutamate (ER.SFLTAPQTEYR) in the two sequences. *In silico* assessment also supports choosing the sequence SFLTAPQTEYR as a more favourable standard peptide.

UGT2B4. Both peptide sequences representative of this enzyme are expected to suffer from missed cleavage due to proximity to glutamate residues in the two sequences (FSPGYAIEK, EER.ANVIASALAK). The sequence ANVIASALAK is expected to have better detectability and a more favorable fragmentation pattern, which is expected to facilitate quantification using this peptide.

UGT2B7. The peptide sequence ADVWLIR is less favorable than TILDELIQR due to several factors. The digestion efficiency is expected to be compromised by the presence of an aspartate (D) in close proximity to the cleavage site, and the presence of a tryptophan (W) within the sequence can lead to instability due to oxidation. The short sequence is predicted to lead to poor detectability under LC-MS conditions and only a small number of targetable transitions. It is also isobaric to VSVWLLR (UGT1A6).

UGT2B15. The peptide sequence WIYGVSK is expected to suffer from instability due to oxidation at the tryptophan residue (W), and poor detectability under MS conditions with only few transitions available for selection. SVINDPVYK is expected to suffer from non-enzymatic hydrolysis at the DP peptide bond. Both peptide sequences are susceptible to missed cleavage due to close proximity of enzyme cleavage sites to acidic residues (SVINDPVYK.E and DR.WIYGVSK). However, the sequence SVINDPVYK was selected for predicted better detectability and fragmentation pattern.

2.2 Effects of systematic appraisal on UGT enzyme abundance and correlation with activity

A summary of the effects of analysis optimization is shown in **Supplemental Table 1**. The case of each enzyme is discussed below.

UGT1A1. Although previously reported data showed good correlation for UGT1A1 abundance and activity, the data analysis strategy was also applied to data related to this enzyme. For UGT1A1, the peptide selection changed based on the selection criteria. In our initial analysis, preference was given to the peptide that returned higher ratios (TYPVPFQR), this view was since revised. **Table 1** shows the selected sequence (DGAFYTLK) and **Supplemental Figure 1** shows the elution profiles of both peptides. Quality control runs also returned more favorable inter-day variability for the selected peptide (Achour et al., 2017). Appraisal of fragments showed that the short fragment (y_4) was not specific (with potential isobaric and isomeric interference), and therefore was excluded from analysis. These changes in the monitored transitions (peptide and fragments) led to little change in mean abundance from 33.6 to 34.1 pmol mg^{-1}, no change in correlation with activity (Rs=0.78, p<0.001), but improved scatter of the data (R^2=0.57), in this case mainly due to the absence of an outlier in previously reported data (**Figure 3**). Correction for standard purity had little effect on abundance (5% change in mean abundance) and correlation (Rs=0.78, p<0.001, R^2=0.58). Correlation and scatter further improved due to consistent normalization to BCA-measured fractional protein mass (Rs=0.87, p<0.001, R^2=0.73), while mean abundance changed moderately to 32.2 pmol mg^{-1}.

UGT1A3. The case of UGT1A3 was complicated due to the low quality of the only peptide used for quantification, although theoretical and in silico parameters indicated it should be a suitable choice (**Table 1**). This peptide returned low quality elution profiles (**Supplemental Figure 1**), on the most hydrophobic side of the chromatogram, relatively low intensity signals with low signal-to-noise ratios. This necessitated looking at the fragments more carefully. The lowest quality elution profile pertained to one fragment (y_5), which consistently reported low quality QconCAT signal and higher light:heavy peptide ratios (5-fold on average) and represented a non-specific fragment; this fragment was excluded from analysis. Only the longest fragment (y_7), that returned more consistent quantification ratios with the highest quality elution profile, was used. The mean abundance changed from 123.1 to 27.8 pmol mg^{-1}. This example shows a case where using strict filters and appraisal of monitored fragments can have a substantial effect on protein quantification. Although correlation with activity improved with this change (from Rs=0.64 to Rs=0.80, p<0.001), scatter did not improve substantially (R^2=0.30 to 0.47). Normalization to the same fractional protein data improved scatter in abundance-activity correlation (Rs=0.85, p<0.001, R^2=0.71), with mean abundance changing to 26.3 pmol mg^{-1}. The methods used to quantify UGT1A3 using the current QconCAT remain problematic and new methods should be developed for this enzyme.

UGT1A4. Both peptide choices representing UGT1A4 required chemical modification (at the level of cysteines) and the modified peptide was monitored. The peptide selected in previous analysis (YIPCDLDFK) was shown to be more favourable than the alternative peptide based on the theoretical and in silico criteria. However, one of the fragments (y_5) used in previous analysis was excluded due to its sequence not containing the modified cysteine, being less specific and returning higher ratios than longer fragment sequences (y_6, y_7) . This assessment led to a small decrease in UGT1A4 mean abundance from 58.0 to 47.5 pmol mg^{-1} and to improvement in correlation (Rs=0.56, p=0.004), with high level of scatter in the data (R^2=0.24). There was little change in correlation due to correction for standard purity (Rs=0.56, p=0.005, R^2=0.26). Applying normalization to the data resulted in improved scatter (Rs=0.75, p<0.001, R^2=0.58), with mean abundance changing to 46.2 pmol mg^{-1}. Protein-protein expression inter-correlations identified included the pair UGT1A4/UGT2B4 (Rs=0.63, p=0.001, R^2=0.45) (**Supplemental Figure 5**, **Supplemental Table 3**), which was also seen with data generated using SIL-peptides in the larger sample set (n=60) as reported previously (Achour et al., 2017). The methods for the quantification of UGT1A4 may still need optimization by choosing a better performing peptide that does not require modification.

UGT1A6. The case for UGT1A6 highlighted the importance of avoiding isobaric sequences. The peptide used previously (VSVWLLR) had the same parent mass, fragment masses and retention time as the sequence for UGT2B7 (ADVWLIR), which meant interference between the two peptides could not be avoided and led to over-estimating both protein quantities. **Supplemental Figure 1** shows the overlap between the two peaks. This meant that the abundance data were inevitably exaggerated in the case of UGT1A6. In the new selection (SFLTAPQTEYR), the short fragment y_6 was also excluded due to potential isobaric interference. The new peptide selection reported a reduction in the mean abundance of UGT1A6 from 107.1 to 16.6 pmol mg^{-1} (which teased out UGT2B7 abundance levels), with improvement in the level of correlation with activity (Rs=0.52, p=0.01, R^2=0.31). There was no change in correlation due to correcting for standard purity. After normalization, the mean abundance changed to 15.6 pmol mg^{-1}, which is more in line with data generated using SIL standards (Achour et al., 2017b) and the correlation further improved (Rs=0.67, p<0.001, R^2=0.48).

UGT1A9. The case of UGT1A9 was similar to that of UGT1A3; the quantification was based on only one peptide which was highly hydrophobic and had low quality LC-MS profile (**Supplemental Figure 1**). The selected sequence was of low quality, prone to degradation and required chemical modification (**Table 1**). Similar to the case for UGT1A3, the change in method was based on fragment choice. The sequence contained a DP domain which is prone to cleavage in acidic conditions. Therefore, any fragments longer than y_{11} were deemed less stable and represented poor reporters. Using only this one transition led to little change in mean abundance from 40.0 to 39.0 pmol mg^{-1}, which did not have much effect on correlation with

activity, as this remained weak, statistically non-significant, with significant scatter (Rs=0.20, p=0.33, R^2=0.07). Correction for purity of standard did not change the correlation (Rs=0.20, p=0.33, R^2=0.07). The main contributor to the improved correlation was the abundance normalization, which led to a moderate, statistically significant relationship (Rs=0.47, p=0.02), though with some level of scatter (R^2=0.34). The choice of peptide and quantification methods for UGT1A9 using the current QconCAT remain sub-optimal and new methods are required.

UGT2B4. The peptide used for the UGT2B4 quantification remained the same as the previous assessment after applying the selection criteria (ANVIASALAK). Assessment of elution profiles showed that one fragment (y_8) gave split peaks and lower quality profiles. Appraisal of fragment y_6 showed potential isobaric interference. Quantification based on one fragment resulted in a change in mean abundance from 70.8 to 53.9 pmol mg^{-1}. Correction for incorporation did not change mean levels significantly (5% change). Abundance normalization changed the mean abundance slightly to 51.6 pmol mg^{-1}. There were no activity measurements for this enzyme. Comparison with SIL-based data (mean abundance, 39.3 pmol mg^{-1}) showed good expression correlation (**Supplemental Figure 4**).

UGT2B7. The abundance of UGT2B7 was measured using the same peptide used in our previous report (TILDELIQR) due to the reason described above (see UGT1A6 results). One fragment (y_5) was excluded from quantification due to reporting higher ratios, having a non-unique sequence and returning split peaks on the chromatogram (**Supplemental Figure 1**). This assessment led to little change in mean abundance from 82.9 to 78.7 pmol mg^{-1} and slight improvement in correlation from (Rs=0.40, p=0.045, R^2=0.30) to (Rs=0.48, p=0.02, R^2=0.49), which was still considered moderate. Correction for purity of standard did not have a significant effect on mean abundance or correlation with activity (Rs=0.48, p=0.02, R^2=0.48). Normalization of abundance resulted in improvement mainly in the scatter of the data (Rs=0.53, p=0.01, R^2=0.60) with little change in mean abundance 77.3 pmol mg^{-1}. Another protein-protein inter-correlation in the abundance dataset included the pair UGT2B7/UGT2B15 (**Supplemental Figure 5**, **Supplemental Table 3**) (Rs=0.62, p=0.001, R^2=0.48), in line with our previous report (Achour et al., 2017).

UGT2B15. Peptide choice was changed based on the selection criteria to SVINDPVYK (**Table 1**). The fragment y_4 was also excluded from the analysis due to its short sequence, and only the fragments deemed more specific (y_6 and y_7) were used for quantification. These changes led to a decrease in mean abundance from 62.1 to 45.2 pmol mg^{-1} and abundance-activity correlation changed from (Rs=0.35, p=0.09, R^2=0.14) to (Rs=0.52, p=0.01, R^2=0.29), representing more improvement in correlation than in scatter of the data. Correction for purity of standard did not affect mean abundance or activity correlation significantly

(Rs=0.50, p=0.01, R^2=0.29). Abundance normalization led to more substantial improvement in activity correlation (Rs=0.65, p<0.001, R^2=0.60).

2.3 Cross-laboratory evaluation of UGT abundance measurement

Supplemental Figures 3 and **4** show comparison of UGT abundance data acquired in two independent laboratories using two proteomic methodological workflows (gel-based sample preparation with QconCAT proteomic analysis *vs* in-solution sample preparation with SIL peptide-based proteomic analysis). With the three types of correction applied, the QconCAT approach now correlates well with the quantification achieved with the SIL approach in the cases of UGTs 1A1, 1A3, 1A4 and 2B4. The exception is UGT1A3 as shown in **Supplemental Figure 3**; although the readings from the two laboratories are correlated, the scale of abundance still reflects a significant cross-laboratory disparity.

2.4 Abundance-activity and abundance-abundance cross-relationships

Supplemental Table 2 shows correlation of UGT activity rates with abundance levels after optimization of analysis (**Figure 4** in the manuscript), and **Supplemental Table 3** shows expression correlations between UGT protein levels (**Supplemental Figure 5**).

2.5 QconCAT-based methods after optimization

Supplemental Table 4 shows optimized methods for the enzymes that can be adequately quantified using the current QconCAT, and the enzymes for which new methods are required.
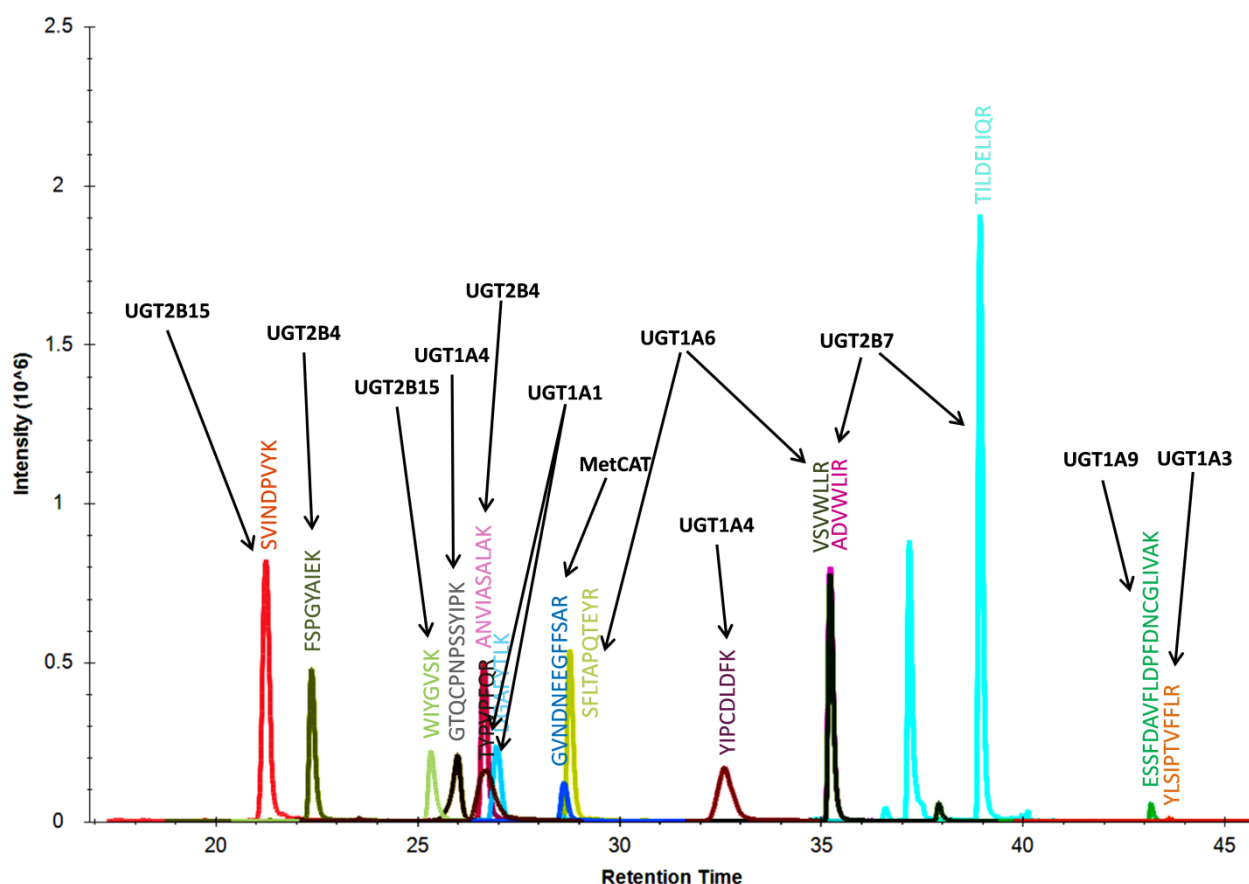
Supplemental Figure 1 Elution profiles of UGT Q-peptides analyzed in the same LC-MS/MS assay (sample HH06). Peptide sequences, intensities, retention times (in minutes) and the UGT enzymes they represent are shown. The figure shows the overlap between peaks for the isobaric sequences VSVWLLR (UGT1A6) and ADVWLIR (UGT2B7), rendering them less useful in quantification experiments. The figure also shows the two single peptide sequences YLSIPTVFFLR (UGT1A3) and ESSFDAVFLDPFDNCGLIVAK (UGT1A9), which were of sub-optimal hydrophobicity and eluted late in the LC run with lower quality elution profiles characterised by low signal-to-noise ratio at the MS and MS/MS levels

Brahim Achour, Alyssa Dantonio, Mark Niosi, Jonathan J. Novak, Zubida M Al-Majdoub, Theunis C. Goosen, Amin Rostami-Hodjegan and Jill Barber
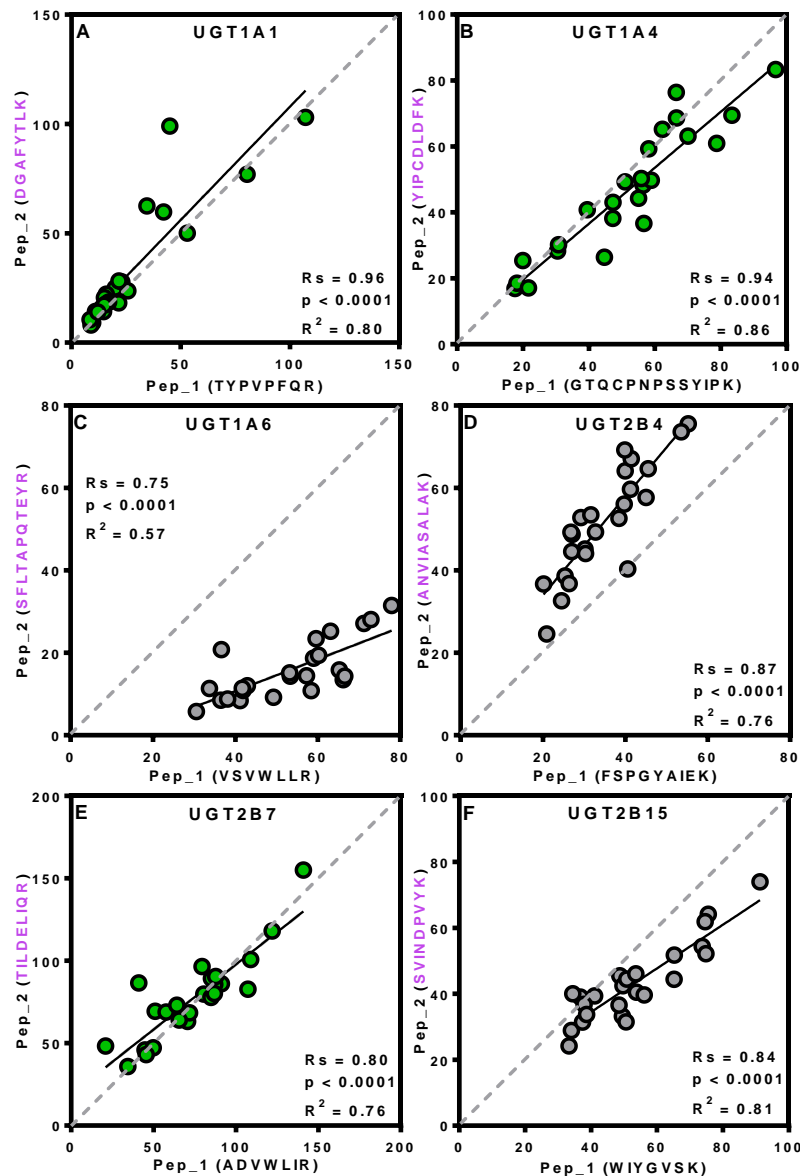
Supplemental Figure 2 Correlation of UGT abundance values measured using the two QconCAT peptides representing UGT1A1 (A), UGT1A4 (B), UGT1A6 (C), UGT2B4 (D), UGT2B7 (E) and UGT2B15 (F) after optimization. Although Statistical analysis showed good correlations between abundances related to the pairs of peptides, there were significant differences identified for the abundance levels of UGTs 1A6, 2B4 and 2B15 (gray data points), with the largest difference observed with UGT1A6 (Mann-Whitney U-test). Peptide sequences highlighted in purple font were used for subsequent abundance measurement in this report (based on criteria shown above). Units of abundance measurements: pmol mg^{-1} HLM protein. Continuous lines represent lines of regression and dashed lines are lines of unity. A number of outlier measurements were identified for TYPVPFQR_UGT1A1 (2 outliers), VSVWLLR_UGT1A6 (1 outlier) and WIYGVSK_UGT2B15 (1 outlier)

Data Generated by Quantitative LC-MS Proteomics Are Only the Start and Not the Endpoint: Optimization of QconCAT-Based Measurement of Hepatic UDP-Glucuronosyltransferase Enzymes with Reference to Catalytic Activity

Brahim Achour, Alyssa Dantonio, Mark Niosi, Jonathan J. Novak, Zubida M Al-Majdoub, Theunis C. Goosen, Amin Rostami-Hodjegan and Jill Barber
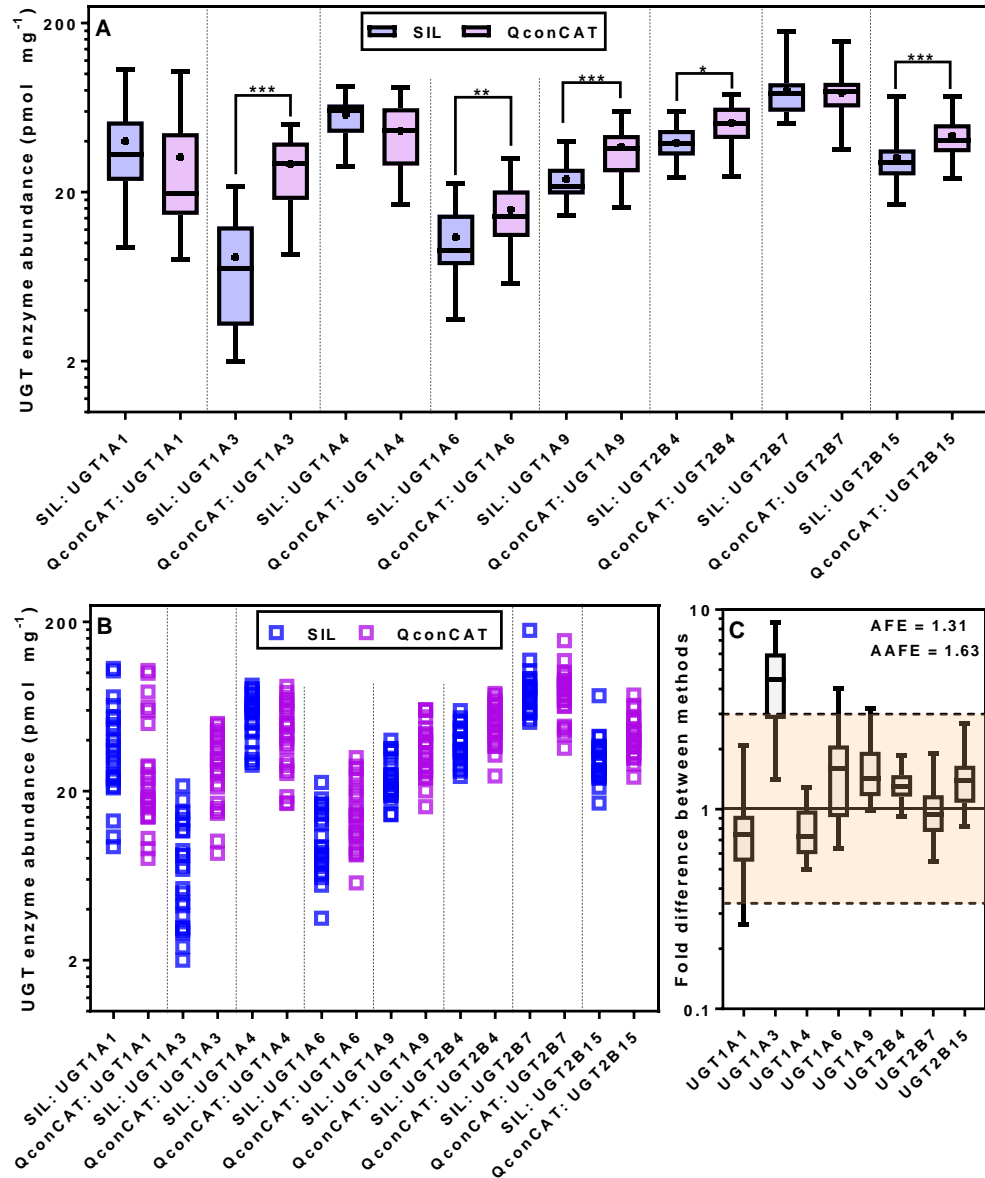
Supplemental Figure 3 Cross-laboratory evaluation of UGT abundance measurements using stable isotope-labeled (SIL) peptide standards and quantification concatemer (QconCAT) standard: Box and whiskers plot of the abundance measurements (n=24) of UGT enzymes quantified by the two methods (A) with the individual values shown in panel (B). Fold difference (fold error) of matched values (i.e., $\left[x_{QconCAT,i}/x_{SIL,i} \right]$ for each enzyme i) is shown in panel (C). The shaded area in panel (C) represents values within 3 fold, to represent inter-changeable abundance data. In panels (A) and (C), the boxes represent the 25th and the 75th percentiles, the whiskers represent the minimum and maximum values and the bars represent the medians. In panel (A), the + sign represents the arithmetic mean. Differences were tested using Mann-Whitney rank order U-test: **, $p < 0.01$; ***, $p < 0.001$. In panel (C), AFE is the average fold error and AAFE is the absolute average fold error. Units of abundance measurements are pmol mg^{-1} HLM protein
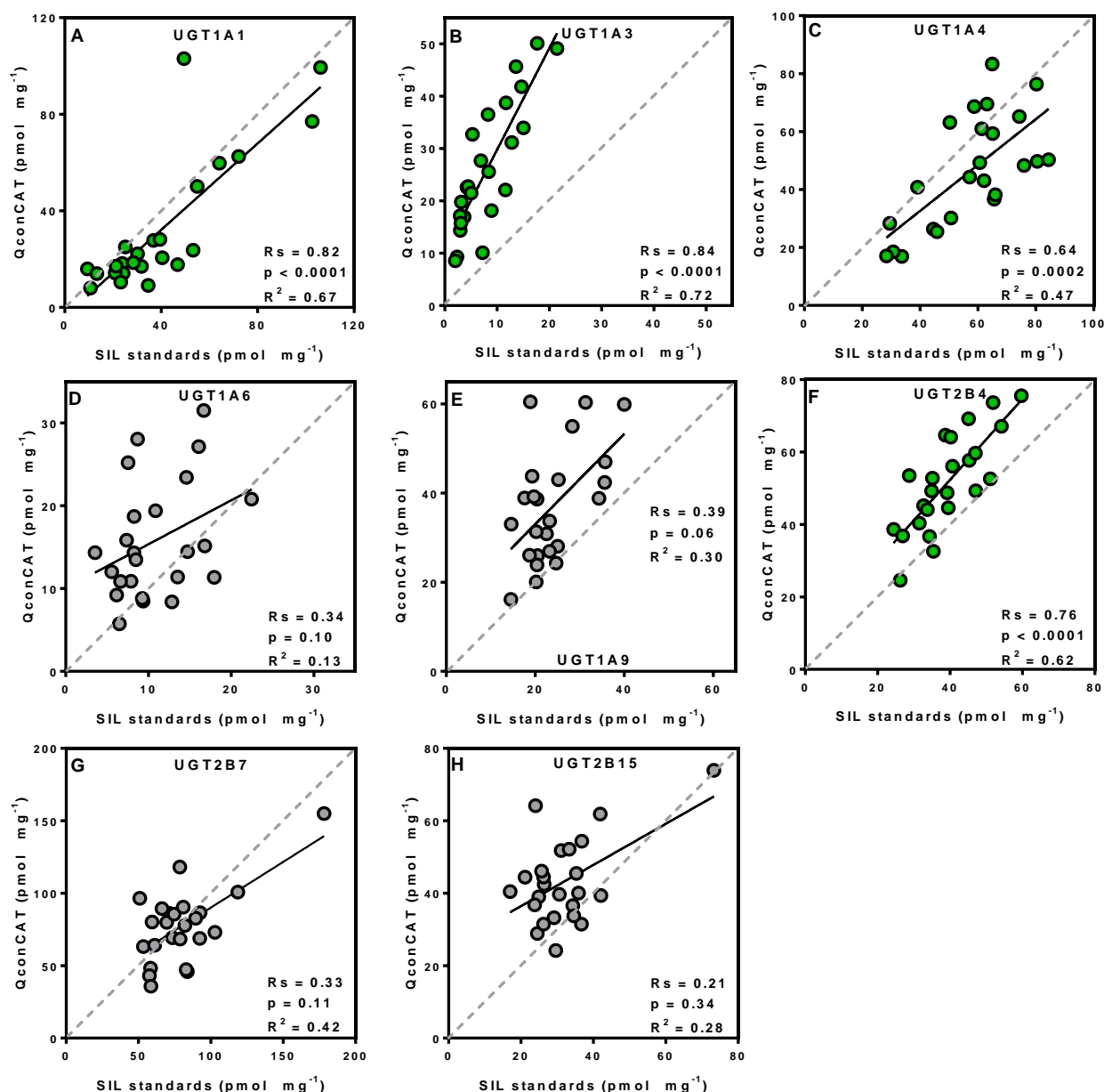
Supplemental Figure 4 Correlation between individual protein abundance measurements (n=24) of UGTs 1A1 (A), 1A3 (B), 1A4 (C), 1A6 (D), 1A9 (E), 2B4 (F), 2B7 (G) and 2B15 (H) using two proteomic methodologies (SIL vs QconCAT) after optimization of QconCAT data analysis. Strong correlation was observed for UGTs 1A1, 1A3, 1A4 and 2B4 (shown in green). SIL, stable isotope-labeled peptide standards; QconCAT, quantitative concatemer standard; Rs, Spearman rank order correlation coefficient
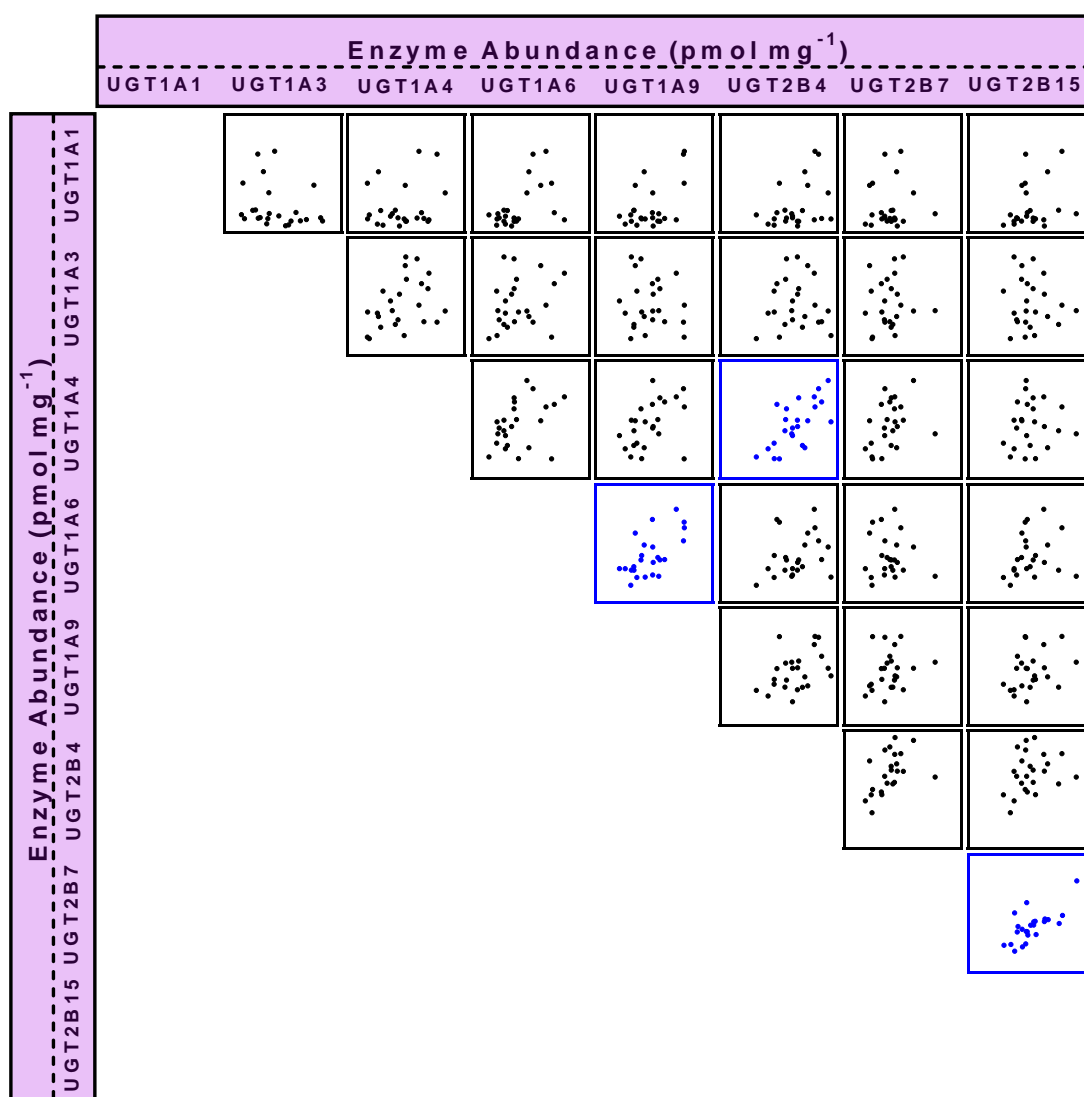
Supplemental Figure 5 Correlation matrix of individual protein abundances of UGT enzymes (abundance vs abundance) using QconCAT methodology (n=24). Strong, statistically significant correlations are shown in blue. Units of abundance measurements are pmol mg-1 HLM protein. Supplemental Table 3 shows the statistical analysis used to generate the abundance-activity correlation matrix.

Data Generated by Quantitative LC-MS Proteomics Are Only the Start and Not the Endpoint: Optimization of QconCAT-Based Measurement of Hepatic UDP-Glucuronosyltransferase Enzymes with Reference to Catalytic Activity

Brahim Achour, Alyssa Dantonio, Mark Niosi, Jonathan J. Novak, Zubida M Al-Majdoub, Theunis C. Goosen, Amin Rostami-Hodjegan and Jill Barber

Supplemental Table 1 Comparison of QconCAT-based UGT measurements before and after optimization of data analysis

Enzyme	Before optimization of analysis			After optimization of analysis			Bias statistics			
	Mean ± SD (%CV) [a] [pmol mg⁻¹]	Range (fold variation) [b] [pmol mg⁻¹]	Correlation with activity (Rs, p-value; R²) [c]	Mean ± SD (%CV) [a] [pmol mg⁻¹]	Range (fold variation) [b] [pmol mg⁻¹]	Correlation with activity (Rs, p-value; R²) [c]	Overall %RE [d] AFE [e] AAFE [e]	%RE [d] (peptide/fragment selection)	%RE [d] (protein mass)	%RE [d] (label incorporation)
UGT1A1	33.6 ± 34.0 (101%)	8.9–137.9 (16)	**0.79, <0.0001; 0.30**	32.2 ± 27.8 (86%)	8.0 – 103.0 (13)	**0.87, <0.0001; 0.73**	-50.2% –+227.1% 0.98 1.33	-24.6%–+221.1%	-49.3%–+44.6%	+0.1%–+8.6%
UGT1A3	123.1 ± 122.3 (99%) [f]	26.9–487.7 (18)	**0.64, 0.001; 0.30**	26.3 ± 12.4 (47%) [f]	8.6 – 50.1 (6)	**0.85, <0.0001; 0.71**	-91.5% – -0.3% 0.30 3.41	-93.1%– -14.7%	-49.3%–+44.6%	+1.4%–+9.3%
UGT1A4	58.0 ± 24.8 (43%)	14.4–105.6 (7)	0.19, >0.05; 0.01	46.2 ± 19.2 (42%)	16.9 – 83.3 (5)	**0.75, <0.0001; 0.58**	-62.4% –+88.1% 0.84 1.42	-60.5%–+64.9%	-49.3%–+44.6%	+2.1%–+9.7%
UGT1A6	107.1 ± 80.3 (75%) [f]	31.6–285.4 (9)	0.25, >0.05; 0.12	15.8 ± 7.0 (45%) [f]	5.7 –31.5 (6)	**0.67, 0.0003; 0.48**	-91.8% – -60.7% 0.17 6.07	-91.3%– -60.4%	-49.3%–+44.6%	+1.1%–+8.6%
UGT1A9	40.0 ± 23.7 (59%) [f]	13.5–122.6 (9)	-0.10, >0.05; 0.01	37.0 ± 12.8 (35%) [f]	16.2 – 60.5 (4)	*0.47, 0.02; 0.34*	-51.8%–+160.9% 1.00 1.40	-48.4%–+105.6%	-49.3%–+44.6%	+1.3%–+8.6%
UGT2B4	70.8 ± 32.3 (46%)	22.8–135.8 (6)	–[g]	51.6 ± 13.3 (26%)	24.6 – 75.6 (3)	–[g]	-56.0 %–+102.1% 0.78 1.45	-61.9%–+64.6%	-49.3%–+44.6%	+2.7%–+9.6%
UGT2B7	82.9 ± 36.1 (44%)	33.0–162.9 (5)	*0.40, 0.045; 0.30*	77.3 ± 25.9 (34%)	35.9 – 155.0 (4)	**0.53, 0.007; 0.60**	-53.7%–+162.2% 0.98 1.30	-29.1%–+112.5%	-49.3%–+44.6%	+2.4%–+9.4%
UGT2B15	62.1 ± 31.5 (51%)	18.3–130.2 (7)	0.35, >0.05; 0.14	43.2 ± 11.8 (27%)	24.2 – 73.9 (3)	**0.65, 0.0005; 0.60**	-42.14% –+147.9% 0.77 1.54	-62.1%–+102.5%	-49.3%–+44.6%	+4.3%–+8.6%

[a] Coefficients of variation are calculated using the standard deviation relative to the arithmetic mean ($\%CV = \frac{SD_i}{\bar{x}_i} \cdot 100\%$) for each enzyme i, units of measurement: pmol enzyme per mg microsomal protein

[b] Fold variation ratios are calculated based on the range (Fold variation $= Max_i/Min_i$) for each enzyme i

[c] Rs, Spearman rank order correlation coefficient; p, p-value of Spearman correlation test; R^2, regression correlation coefficient; **bold font** shows strong and significant abundance-activity correlations, ***bold italic*** shows moderate abundance-activity correlations

[d] Relative error between measurements is calculated ($\%RE = \frac{(x_{1,i}-x_{2,i})}{x_{2,i}} \cdot 100\%$) for one measurement relative to the other for each enzyme i

[e] Average fold error (AFE) allows underestimations and overestimations to cancel one another resulting in a measure of bias (pattern of difference), whereas the absolute average fold error (AAFE) in measurements is calculated by converting all log fold errors to positive values resulting in a measure of scatter or spread of measurements; the closer these two measures to 1, the lower the bias and scatter in measurements
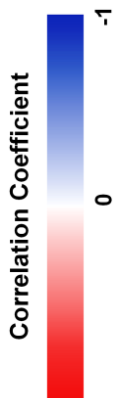
[f] Statistically significant difference between the datasets corresponding to the same enzyme using Mann-Whitney U-test

[g] Catalytic activity of UGT2B4 was not determined in these HLM samples

Data Generated by Quantitative LC-MS Proteomics Are Only the Start and Not the Endpoint: Optimization of QconCAT-Based Measurement of Hepatic UDP-Glucuronosyltransferase Enzymes with Reference to Catalytic Activity

Brahim Achour, Alyssa Dantonio, Mark Niosi, Jonathan J. Novak, Zubida M Al-Majdoub, Theunis C. Goosen, Amin Rostami-Hodjegan and Jill Barber

Supplemental Table 2 Correlation matrix of QconCAT-derived individual UGT enzyme abundances (n=24) with activity rates (abundance vs activity). Factors considered in assessing correlations: Spearman correlation coefficient (Rs), significance of correlation and scatter of the data (R^2)
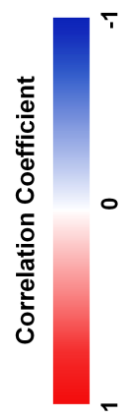
	UGT1A1	UGT1A3	UGT1A4	UGT1A6	UGT1A9	UGT2B7	UGT2B15	UGT2B4
EST (UGT1A1)	**Rs=0.87** **p<0.0001** **R^2=0.73**	Rs=-0.41 p=0.05 R^2=0.06	Rs=0.01 p>0.05 R^2=0.11	Rs=0.28 p>0.05 R^2=0.11	Rs=0.15 p>0.05 R^2=0.14	Rs=-0.06 p>0.05 R^2=0.00	Rs=0.05 p>0.05 R^2=0.01	Rs=0.20 p>0.05 R^2=0.15
CDCA (UGT1A3)	Rs=-0.21 p>0.05 R^2=0.00	**Rs=0.85** **p<0.0001** **R^2=0.71**	Rs=0.41 p=0.05 R^2=0.11	Rs=0.28 p>0.05 R^2=0.05	Rs=0.14 p>0.05 R^2=0.00	Rs=0.27 p>0.05 R^2=0.04	Rs=0.26 p>0.05 R^2=0.00	Rs=0.09 p>0.05 R^2=0.01
TFP (UGT1A4)	Rs=-0.02 p>0.05 R^2=0.04	Rs=0.49 p=0.02 R^2=0.16	**Rs=0.75** **p<0.0001** **R^2=0.58**	Rs=0.12 p>0.05 R^2=0.01	Rs=0.38 p>0.05 R^2=0.12	Rs=0.42 p=0.04 R^2=0.12	Rs=-0.07 p>0.05 R^2=0.00	Rs=0.38 p>0.05 R^2=0.17
5HTOL (UGT1A6)	Rs=0.33 p>0.05 R^2=0.31	Rs=0.32 p>0.05 R^2=0.09	Rs=0.33 p>0.05 R^2=0.15	**Rs=0.67** **p<0.001** **R^2=0.48**	Rs=0.29 p>0.05 R^2=0.17	Rs=-0.24 p>0.05 R^2=0.04	Rs=-0.22 p>0.05 R^2=0.02	Rs=0.11 p>0.05 R^2=0.03
PRO (UGT1A9)	Rs=-0.04 p>0.05 R^2=0.09	Rs=0.12 p>0.05 R^2=0.00	Rs=0.12 p>0.05 R^2=0.03	Rs=0.27 p>0.05 R^2=0.08	**Rs=0.47** **p=0.02** **R^2=0.34**	Rs=-0.02 p>0.05 R^2=0.00	Rs=0.06 p>0.05 R^2=0.00	Rs=-0.24 p>0.05 R^2=0.00
AZT (UGT2B7)	Rs=0.11 p>0.05 R^2=0.01	Rs=-0.07 p>0.05 R^2=0.02	Rs=-0.22 p>0.05 R^2=0.02	Rs=-0.27 p>0.05 R^2=0.14	Rs=-0.07 p>0.05 R^2=0.00	**Rs=0.53** **p=0.007** **R^2=0.60**	Rs=0.12 p>0.05 R^2=0.19	Rs=0.20 p>0.05 R^2=0.02
OXAZ (UGT2B15)	Rs=0.02 p>0.05 R^2=0.00	Rs=0.17 p>0.05 R^2=0.00	Rs=-0.02 p>0.05 R^2=0.00	Rs=-0.03 p>0.05 R^2=0.00	Rs=-0.03 p>0.05 R^2=0.01	Rs=0.37 p>0.05 R^2=0.35	**Rs=0.65** **p<0.001** **R^2=0.60**	Rs=0.04 p>0.05 R^2=0.00

Correlation Coefficient: -1 (blue) / 0 / 1 (red)

Substrates: EST, β-estradiol; CDCA, chenodeoxycholic acid; TFP, trifluoperazine; 5HTOL, 5-hydroxytryptophol; PRO, propofol; AZT, zidovudine; OXAZ, S-oxazepam

Data Generated by Quantitative LC-MS Proteomics Are Only the Start and Not the Endpoint: Optimization of QconCAT-Based Measurement of Hepatic UDP-Glucuronosyltransferase Enzymes with Reference to Catalytic Activity

Brahim Achour, Alyssa Dantonio, Mark Niosi, Jonathan J. Novak, Zubida M Al-Majdoub, Theunis C. Goosen, Amin Rostami-Hodjegan and Jill Barber

Supplemental Table 3 Correlation matrix of individual protein abundances of UGT enzymes (abundance *vs* abundance) using QconCAT methodology (*n*=24). Factors considered in assessing correlations: Spearman correlation coefficient (Rs), significance of correlation and scatter of the data (R^2)

	UGT1A1	UGT1A3	UGT1A4	UGT1A6	UGT1A9	UGT2B4	UGT2B7	UGT2B15
UGT1A1	-	Rs=-0.37 p>0.05 R^2=0.05	Rs=0.03 p>0.05 R^2=0.04	Rs=0.43 p=0.04 R^2=0.28	Rs=0.21 p>0.05 R^2=0.26	Rs=0.28 p>0.05 R^2=0.15	Rs=0.07 p>0.05 R^2=0.00	Rs=0.27 p>0.05 R^2=0.07
UGT1A3		-	Rs=0.44 p=0.03 R^2=0.15	Rs=0.26 p>0.05 R^2=0.06	Rs=-0.02 p>0.05 R^2=0.01	Rs=0.00 p>0.05 R^2=0.00	Rs=0.16 p>0.05 R^2=0.01	Rs=0.01 p>0.05 R^2=0.01
UGT1A4			-	Rs=0.41 p=0.05 R^2=0.15	Rs=0.50 p=0.01 R^2=0.21	**Rs=0.63 p=0.001 R^2=0.45**	Rs=0.41 p=0.05 R^2=0.14	Rs=0.10 p>0.05 R^2=0.01
UGT1A6				-	**Rs=0.55 p=0.005 R^2=0.39**	Rs=0.32 p>0.05 R^2=0.08	Rs=0.01 p>0.05 R^2=0.01	Rs=0.26 p>0.05 R^2=0.03
UGT1A9					-	Rs=0.43 p=0.04 R^2=0.17	Rs=0.32 p>0.05 R^2=0.05	Rs=0.32 p>0.05 R^2=0.10
UGT2B4						-	Rs=0.56 p=0.004 R^2=0.22	Rs=0.30 p>0.05 R^2=0.07
UGT2B7							-	**Rs=0.62 p=0.001 R^2=0.48**
UGT2B15								-

Correlation Coefficient

-1

0

1

Supplemental Table 4 Enzymes with established QconCAT-based quantification methods after optimization. A new QconCAT (MetCAT2) includes peptides based on performance and validation against catalytic activity.

Enzyme [a]	Peptide sequence	MRM transitions	Comments
UGT1A1	DGAFYTLK	$457.73^{+2}/671.38^{+1}$ (y_5) $457.73^{+2}/742.41^{+1}$ (y_6)	
UGT1A4	YIPCDLDFK [b]	$585.78^{2+}/797.35^{+1}$ (y_6) $585.78^{2+}/894.40^{+1}$ (y_7)	This peptide still requires carbamidomethylation. Other options include: FFTLTAYAVPWTQK and YLSIPAVFFWR, used in MetCAT2.
UGT1A6	SFLTAPQTEYR	$656.83^{2+}/864.42^{+1}$ (y_7) $656.83^{2+}/965.47^{+1}$ (y_8)	Only fragments with long sequences are monitored.
UGT2B4 [c]	ANVIASALAK	$479.29^{2+}/673.42^{+1}$ (y_7)	Only one fragment was shown to be of good quality. Another specific transition using a long fragment (y_9) needs to be validated. Proteomic methods should also be validated with activity data.
UGT2B7	TILDELIQR	$550.82^{2+}/773.42^{+1}$ (y_6) $550.82^{2+}/886.50^{+1}$ (y_7)	
UGT2B15	SVINDPVYK	$517.78^{2+}/735.37^{+1}$ (y_6) $517.78^{2+}/848.45^{+1}$ (y_7)	

[a] Enzymes which still need methods to be developed are: UGTs 1A3, 1A5, 1A7, 1A8, 1A9, 1A10, 2B10, 2B11, and 2B17.

[b] The selection for UGT1A4 needs optimization. The underlined amino acid (cysteine) requires chemical modification prior to analysis.

[c] UGT2B4 still requires validation using activity data and additional transitions for the selected peptide.

References

Achour B, Al-Majdoub ZM, Al Feteisi H, Elmorsi Y, Rostami-Hodjegan A, Barber J (2015) Ten years of QconCATs: Application of multiplexed quantification to small medically relevant proteomes. *International J Mass Spectrom* **391**:93-104.

Achour B, Dantonio A, Niosi M, Novak JJ, Fallon JK, Barber J, Smith PC, Rostami-Hodjegan A and Goosen TC (2017) Quantitative Characterization of Major Hepatic UDP-Glucuronosyltransferase Enzymes in Human Liver Microsomes: Comparison of Two Proteomic Methods and Correlation with Catalytic Activity. *Drug Metab Dispos* **45:** 1102-1112.

Achour B, Russell MR, Barber J and Rostami-Hodjegan A (2014) Simultaneous quantification of the abundance of several cytochrome P450 and uridine 5′-diphospho-glucuronosyltransferase enzymes in human liver microsomes using multiplexed targeted proteomics. *Drug Metab Dispos* **42**:500-510.

Carroll KM, Simpson DM, Eyers CE, Knight CG, Brownridge P, Dunn WB, Winder CL, Lanthaler K, Pir P, Malys N, Kell DB et al. (2011) Absolute quantification of the glycolytic pathway in yeast: deployment of a complete QconCAT approach. *Mol Cell Proteomics* **10**:M111-007633.

Deutsch E W (2010) The peptideatlas project. *Methods Mol Biol* **604**:285-296.

Eyers CE, Lawless C, Wedge DC, Lau KW, Gaskell SJ, Hubbard SJ (2011) CONSeQuence: prediction of reference peptides for absolute quantitative proteomics using consensus machine learning approaches. *Mol Cell Proteomics* **10**:M110-003384.

Fallon JK, Neubert H, Hyland R, Goosen TC, Smith PC (2013) Targeted quantitative proteomics for the analysis of 14 UGT1As and -2Bs in human liver using NanoUPLC-MS/MS with selected reaction monitoring. *J Proteome Res* **12**:4402-4413.

Fenyö D, Eriksson J, Beavis R (2010) Mass spectrometric protein identification using the global proteome machine. *Methods Mol Biol* **673**:189-202.

Käll L, Krogh A, Sonnhammer EL (2007) Advantages of combined transmembrane topology and signal peptide prediction—the Phobius web server. *Nucleic Acids Res* **35**:W429-W432.

Kamiie J, Ohtsuki S, Iwase R, Ohmine K, Katsukura Y, Yanai K, Sekine Y, Uchida Y, Ito S, Terasaki T (2008) Quantitative Atlas of membrane transporter proteins: development and application of a highly sensitive simultaneous LC/MS/MS method combined with novel in-silico peptide selection criteria. *Pharm Res* **25**:1469-1483.

Kuster B, Schirle M, Mallick P, Aebersold R (2005) Innovation: Scoring proteomes with proteotypic peptide probes. *Nat Rev Mol Cell Biol* **6**:577-583.

Lawless C and Hubbard SJ (2012) Prediction of missed proteolytic cleavages for the selection of surrogate peptides for quantitative proteomics. *OMICS* **16**:449-456.

Mallick P, Schirle M, Chen SS, Flory MR, Lee H, Martin D, Ranish J, Raught B, Schmitt R, Werner T, Kuster B, Aebersold R (2007) Computational prediction of proteotypic peptides for quantitative proteomics. *Nat Biotechnol* **25**:125-131.

Pratt JM, Simpson DM, Doherty MK, Rivers J, Gaskell SJ, Beynon RJ (2006) Multiplexed absolute quantification for proteomics using concatenated signature peptides encoded by QconCAT genes. *Nat Protocols* **1**:1029-1043.

Data Generated by Quantitative LC-MS Proteomics Are Only the Start and Not the Endpoint: Optimization of QconCAT-Based Measurement of Hepatic UDP-Glucuronosyltransferase Enzymes with Reference to Catalytic Activity
Brahim Achour, Alyssa Dantonio, Mark Niosi, Jonathan J. Novak, Zubida M Al-Majdoub, Theunis C. Goosen, Amin Rostami-Hodjegan and Jill Barber

20